An assessment of phylogenetic tools for analyzing the interplay between interspecific interactions and phenotypic evolution

Drury, J.P.[1,2*], Grether, G.F.[2], Garland, Jr., T.[3], & Morlon, H.[1]

[1]Institut de Biologie, École Normale Supérieure, CNRS UMR 8197, 75005 Paris, France
[2]Department of Ecology & Evolutionary Biology, University of California, 621 Charles E. Young Dr. S, Los Angeles, CA 90095-1606, USA
[3]Department of Biology, University of California, Riverside, CA 92521, USA

*Corresponding author:
druryj@ucla.edu
(424) 362-6230
621 Charles E. Young Dr. S
Los Angeles, CA 90095-1606, USA

Running head: PHYLOGENETIC TESTS ON SPECIES-PAIR DATASETS

Abstract

Much ecological and evolutionary theory predicts that interspecific interactions often drive phenotypic diversification and that species phenotypes in turn influence species interactions. Several phylogenetic comparative methods have been developed to assess the importance of such processes in nature; however, the statistical properties of these methods have gone largely untested. Here, we assess the performance of available comparative approaches for analyzing the interplay between interspecific interactions and species phenotypes. We find that currently used statistical methods largely fail to detect the impact of interspecific interactions on trait evolution, that sister taxa analyses often erroneously detect character displacement where it does not exist, and that recently developed process-based models have more satisfactory statistical properties. In weighing the strengths and weaknesses of different approaches, we hope to provide a clear guide for empiricists testing hypotheses about the reciprocal effect of interspecific interactions and species phenotypes and to inspire further development of process-based models.

Keywords: character displacement, competition, interspecific interactions, phylogenetic comparative methods, trait evolution

Interactions between species are a fundamental aspect of life on earth, and understanding the evolutionary and ecological consequences of such interactions are a central goal of many classical theoretical frameworks in ecology and evolutionary biology. Identifying both the predictors of interspecific interactions and the consequences of such interactions for diversification and coexistence is thus an important contemporary research area, with strong implications for conservation biology.

Several phylogenetic comparative methods have been deployed with the goal of elucidating how interspecific interactions drive (or are driven by) character evolution, but the reliability and efficacy of these methods remain largely untested. Here we focus on methods used to study interactions between closely related species (e.g., members of the same family) that arise from similarity in morphology, signaling traits or habitat (Brown and Wilson 1956; Schluter 2000; Pfennig and Pfennig 2009), rather than on community-wide interactions and interaction networks (Webb et al. 2002; Rezende et al. 2007; Cavender-Bares et al. 2009; Cadotte et al. 2013).

Classical character displacement theory (Brown and Wilson 1956; Grether et al. 2009; Pfennig and Pfennig 2009) predicts that, where heterospecifics compete, selection should favor divergence in the traits responsible for competition, until lineages in sympatry no longer compete intensely. In a seminal example, selection resulting from exploitative competition between medium and large ground finches (*Geospiza fortis* & *G. magnirostris*) has driven bill size divergence on Daphne Major in the Galápagos (Grant and Grant 2006). Investigators who conduct comparative studies of divergent character displacement often test for a relationship between biogeographic overlap and trait dissimilarity, predicting that coexisting species will be more phenotypically divergent than non-coexisting ones. Recent studies on *Bicyclus* butterflies and *Euglossa* bees, for example, show that male chemical cues are more distinct between sympatric species than allopatric species, suggesting that reproductive character displacement has driven signal divergence in these taxa (Bacquet et al. 2015; Weber et al. 2016).

Interspecific interactions can also lead to convergent, rather than divergent, character displacement (Cody 1969, 1973; Grant 1972; Grether et al. 2013). Agonistic character displacement theory (Grether et al. 2013) predicts convergence in traits mediating interspecific aggression when species compete strongly for the same resources. In other words, between-species similarity in resource use may make interspecific territoriality adaptive, resulting in subsequent convergence in signaling traits involved in mediating territorial interactions (e.g., song in ovenbirds, Tobias *et al.* 2014). Therefore, tests of convergent character displacement typically test the prediction that sympatric lineages are more phenotypically similar than allopatric ones. Because sympatric similarity can also result from convergence to local conditions (e.g., habitat, climate), it is important for empiricists to account for abiotic factors in tests of character convergence.

In some instances, rather than identifying the effect of species interactions on trait evolution, empiricists aim to identify traits that mediate particular pairwise interactions, such as hybridization or interspecific aggression. In this case, investigators test for a relationship between the measured interactions and trait similarity. Recent studies on New World warblers (Parulidae), for example, show that hybridization occurs more often between species with similar songs and that interspecific territoriality occurs more often between species that share similar plumage and territorial song phenotypes (Willis et al. 2014; Losin et al. 2016).

Regardless of the biological question, a particularity of comparative tests aimed at understanding the interplay between interspecific interactions and species phenotypes is that they

largely involve testing correlations between pairwise data (e.g. range overlap, phenotypic similarity, frequency of hybridization). In contrast, most phylogenetic comparative methods have been developed and tested on tip data (e.g. range size, morphological trait values), and the statistical properties of methods adapted to handle pairwise data (Box 1) have gone untested (but see Harmon & Glor 2010). Furthermore, species interactions are inherently affected by the biogeographic history of dispersal and speciation in an evolving clade and the resulting patterns of range overlap. Patterns of trait dissimilarity between sympatric lineages—the classic test of character displacement—may actually be the null expectation if allopatric speciation is the norm, because then sympatric species pairs will tend to share more distant common ancestors than allopatric species pairs do (Weir and Price 2011; Tobias et al. 2014).

Here, we apply the main phylogenetic comparative methods that investigators use to test hypotheses about interactions between closely related lineages and phenotypes (Box 1, Fig. 1) to datasets simulated under different evolutionary histories of speciation, dispersal, species interactions, and trait evolution. We then compare the efficacy of these methods, discuss the relative merits of each, and outline directions for future research.

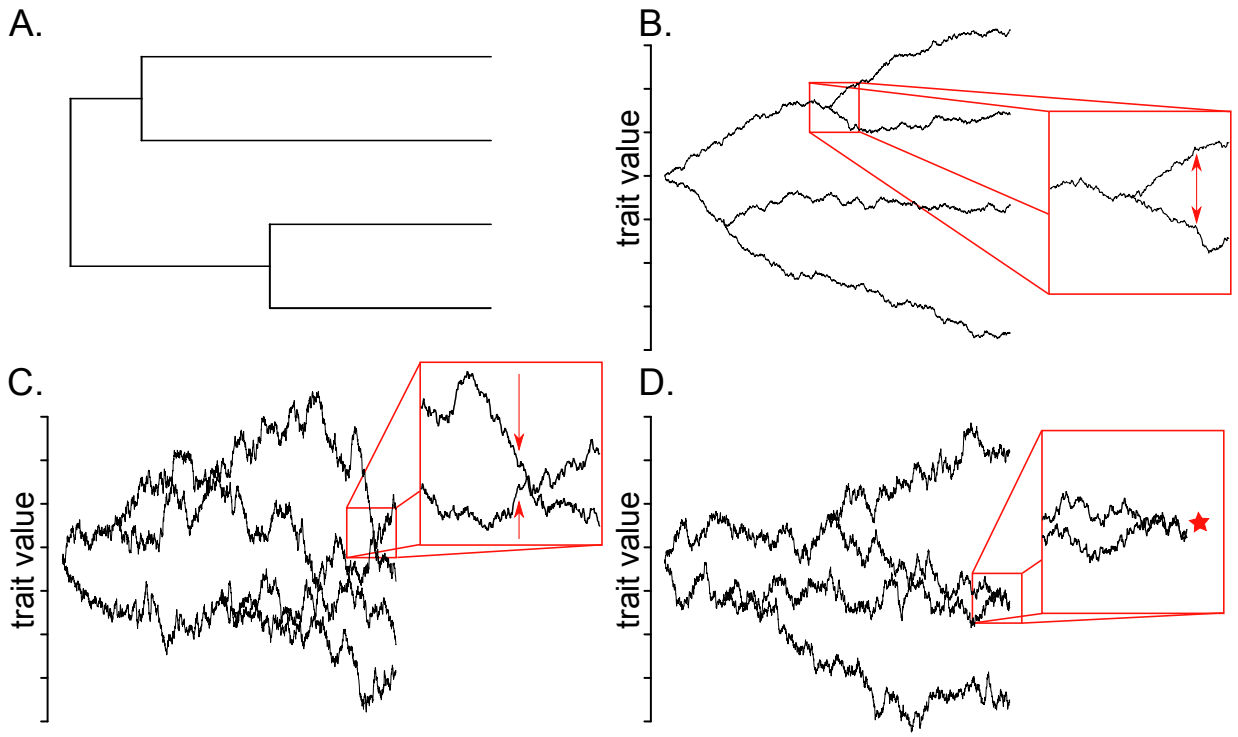

Figure 1. Schematic examples of the processes examined in our simulation study. A. Phylogeny along which the trait evolves. B. A trait evolving via divergent character displacement, C. A trait evolving via convergent character displacement, and D. A species interaction that exists at present due to pairwise trait similarity. For simulation details, see *Supplementary Methods*.

METHODS

We compared the performance of different phylogenetic comparative methods by measuring the statistical power (e.g., probability of detecting divergence when divergence is simulated) and Type I error rate (e.g., probability of detecting an effect of species interactions when such an effect is not simulated) across several scenarios.

Phylogeny and Range Simulations

We jointly simulated trees {# spp. = 20,50,100,150, 200, 250} and biogeographies under the dispersal-extinction-cladogenesis model of biogeographical evolution (i.e., DEC+J, with the inclusion of founder event speciation) in BioGeoBEARS (Ree and Smith 2008; Matzke 2014). For each tree, we started with a single ancestral species occupying one of ten equidistant regions, and simulated trees with constant rates of speciation and local extinction. We considered different biogeographic scenarios by varying the rate of dispersal events between ranges ("high" and "low" dispersal; see details in Supplementary Methods) and the probability that speciation events occur in sympatry versus allopatry ("high" and "low" sympatric speciation; Supplementary Methods). Each of these simulations resulted in a phylogeny (the tree of extant species) and its associated biogeography (the set of regions in which each lineage occurred throughout the history of the clade). Lineages were identified as sympatric if they co-occurred in at least one of the ten geographic regions, and allopatric if they did not co-occur in any.

We simulated four biogeographic scenarios (combinations of low or high dispersal and low or high sympatric speciation) for each tree size. The resulting biogeographies span scenarios where sympatric speciation is common and dispersal is low (e.g., lizards on islands) to scenarios where allopatric speciation is the main mode of speciation and dispersal between regions is high (e.g., birds on continents). These parameter combinations produced a range of realistic proportions of sister taxa that are sympatric (Fig. S1A) and a range of realistic differences in age between sympatric and allopatric sister taxa (Pigot & Tobias 2015; Fig S1B).

For each combination of tree sizes and DEC parameter combinations (n = 24), we performed 100 simulations, resulting in a bank of 2,400 trees with associated biogeographies.

Character Displacement

The model.—We simulated a continuous trait under a model in which species' trait values are repelled from (or drawn toward) the trait values of sympatric members of an evolving clade as a function of their phenotypic similarity. We modified the matching competition model (Nuismer & Harmon 2015; Drury *et al*. 2016) such that the mean trait value z_i in lineage i after an infinitesimally small time step dt is described by:

$$z_i(t+dt) = z_i(t) + \psi\big(\theta - z_i(t)\big)dt + m\left[\sum_{j\neq i}^{n} \mathbf{A}_{i,j} \times sign\left(z_i(t) - z_j(t)\right) \times e^{-\alpha\left(y_j(t) - y_i(t)\right)^2}\right]dt + \delta$$

(Eq. 1)

where $\psi\big(\theta - z_i(t)\big)$ describes attraction to a single stationary peak (i.e., the Ornstein-Uhlenbeck [OU] model), n is the number of species, δ is a random variable with mean 0 and variance = $\sigma^2 dt$ (the Brownian motion [BM] rate parameter, describing the stochastic component of trait evolution), and **A** is a piecewise-constant matrix representing biogeographical overlap such that

$\mathbf{A}_{i,j}$ equals 1 if species i and j are sympatric at time t, and 0 otherwise. The "sign" portion determines the relative position of each species in trait space. The α value determines the effect of pairwise similarity in trait y on competition, with large α values biasing the strength of interactions toward species pairs with similar y values; conversely, as α decreases towards zero, all sympatric lineages interact equally. The parameter m represents the magnitude of the effect of competition when two lineages have identical y values (i.e., it provides an upper bound for the deterministic effect of competition). When $m = 0$, this equation reduces to an OU model, whereas positive m values result in pairwise divergence and negative values result in pairwise convergence. When both m and $\psi = 0$, this model reduces to Brownian motion. For additional simulation details, see *Supplementary Methods*.

We use a lineage-based "phenomenological" model for our simulations rather than an individual-based model in order to have the computational ability to produce datasets of a size comparable to those typically used in empirical comparative phylogenetic studies (i.e. often reaching several hundreds of species). A model derived from microevolutionary first principles would generate similar patterns of character displacement and would be much more computationally intensive, therefore largely restricting the range of parameter values that can be studied. For simplicity, this model also omits the effect of a species geographic structure and gene flow between distinct populations resulting from dispersal on the evolution of the mean species phenotype. This simplification is reasonable in the context of our study because there is no reason to expect that it will systematically bias the patterns generated in such a way as to yield different conclusions regarding the performance of the various analytical approaches that we use here.

Divergent character displacement.—We simulated datasets with divergent character displacement by setting $y = z$ in Eq. 1 such that trait divergence is driven by pairwise similarity in that trait. Biologically, this could represent a feeding trait that co-varies with resource use (e.g., bill shape in Galápagos finches, Grant & Grant 2011) and which would be directly affected by interspecific competition. To assess whether each method could detect divergent character displacement when it occurred and did not erroneously detect character displacement when it was absent, we simulated datasets both with repulsion $\{m = 2\}$ and without repulsion $\{m = 0\}$ (see Supplementary Methods). We also simulated datasets with $\{\psi = 2\}$ and without $\{\psi = 0\}$ the OU process. In all simulations, we held σ^2 constant at 0.5, α constant at 1, and both the state at the root (z_0) and the OU optimum (θ) constant at 0.

In additional simulations run only on 100-species trees, we analyzed the effect of both the maximum strength of repulsion $\{m = 0, 1, 2, 10\}$ and, to understand how the opposing forces of repulsion and attraction to an optimum influence analyses, the ratio of attraction to the maximum effect of competition $\{\psi{:}m = 0, 0.2, 0.5, 1\}$ on inferences. As above, these values were arbitrarily chosen based on visual inspection of realized simulations.

For each parameter combination, we simulated 10 datasets for each tree, resulting in 1,000 simulations for each tree size / biogeographic scenario combination.

Convergent character displacement.—We simulated datasets with convergent character displacement under Eq. 1, where the term y represents a trait determining resource use or niche occupation evolving via BM or OU. A species' trait z in this model—a trait used as a territorial signal—is thus attracted most strongly to the signal trait values of sympatric lineages with the most similar resource-use traits. Biologically, this represents a scenario where selection favors

interspecific territoriality—mediated by similarity in territorial signals—because the benefits of excluding heterospecifics are similar to the benefits of excluding conspecifics (Grether et al. 2009). As a species' resource-use trait becomes less similar to that of sympatric species, the strength of attraction decreases to zero.

We simulated resource-use traits under both BM ($\sigma^2_{resource} = 0.5$, $\psi_{resource} = 0$) and OU ($\sigma^2_{resource} = 0.5$, $\psi_{resource} = 2$, $\theta_{resource} = 0$) models. For the signal trait, we simulated datasets both with convergence $\{m = -0.25\}$ and without convergence $\{m = 0\}$. We did not include attraction toward a stable peak for the signal trait (i.e. ψ was held constant at 0). As above, we held $\sigma^2 = 0.5$ and $z_0 = 0$, though we held α constant at 10, since smaller values result in rapid, cladewise convergence in traits. To analyze the effect of the maximum strength of convergence, we ran another set of simulations on 100-species trees varying m $\{m = 0, -0.1, -0.25, -0.5\}$ (see Supplementary Methods). The resource trait (y) and signal trait (z) were modeled as unlinked and genetically uncorrelated.

As above, we simulated 10 datasets for each tree, resulting in 1,000 simulations for each tree size / biogeographic scenario combination.

Predictors of Interspecific Interactions

In some cases, investigators wish to identify which factors explain the occurrence of particular interspecific interactions. For example, investigators may want to understand which traits cause species to hybridize (e.g., Willis et al. 2014). In this scenario, species interactions vary according to phenotypic similarity between sympatric species pairs (i.e., species pairs that could potentially interact). Additionally, and unlike character displacement analyses, predicting the occurrence of interspecific interactions requires treating trait similarity as a predictor variable rather than a response variable. Thus, we generated datasets where the presence of interactions between sympatric taxa depends on pairwise similarity in traits.

Under this scenario, we first evolved a trait along the phylogeny under a BM ($\sigma^2 = 0.5, \psi = 0$) or OU ($\sigma^2 = 0.5$, $\psi = 2$, $\theta = 0$) model. Next, we simulated a second, independently evolving trait ($\sigma^2_{unmeasured} = 1$, $\psi_{unmeasured} = 0$) to represent an unmeasured trait that could cause the interaction of interest. To generate datasets where species interactions depend on similarity in trait space at the present, we created species interactions in the form of a binomial variable by sampling from a binomial distribution with the probability of interaction equal to:

$$P = \frac{e^{(b_1 Dx_1 + b_2 Dx_2)}}{1 + e^{(b_1 Dx_1 + b_2 Dx_2)}}$$

(Eq. S2)

(e.g., Hilbe 2009) where Dx_n is the distance between species at the present (e.g., distance between tip values) in simulated trait n (simulated using fastBM in phytools, Revell 2012), and b_n is the coefficient determining the magnitude of the relationship between the species interaction and similarity in trait n. Trait 1 is the measured, focal trait and trait 2 represents the independently evolving, unmeasured trait. As the effect of b_n on the species interaction depends on the Dx_n distribution, which in turn depends on the total height of the tree, we scaled the trees to a height of one prior to simulating datasets to facilitate comparison of results across trees and parameter space.

To determine the statistical power of each analytical method, we generated species interactions based on similarity in the measured trait ($b_1 = -4$, $b_2 = 0$); to assess the Type I error

253 rate, we simulated species interactions based on similarity in the unmeasured trait ($b_1 = 0$, $b_2 = -$
254 4). To determine the effect of the magnitude of the coefficient determining the relationship
255 between the measured trait and the interactions, we ran another set of simulations on 100-species
256 trees varying b_1 {$b_1 = 0, -2, -4, -6, -8$} and holding $b_2 = -4$. As above, we ran 1,000 simulations
257 for each tree size / biogeographic scenario combination.
258
259 *Phylogenetic Tests*
260 Among our tests of character displacement (both divergent and convergent), the
261 "correlation" tests involved assessing the significance of the relationship between phenotypic
262 similarity and coexistence, using either the "full" dataset (all species pairs) or the "sister taxa"
263 subset obtained by culling sister taxa from trees with ≥150 tips. To the full datasets, we applied
264 standard non-phylogenetic regression analyses that ignore phylogenetic non-independence, the
265 raw and phylogenetically permuted partial Mantel tests, phylogenetic linear mixed models
266 (PLMMs), and the simulation approach (see Box 1, 1-6 and Supplementary Methods). To the
267 sister-taxa datasets, we applied non-phylogenetic regression analyses, PLMMs, the simulation
268 approach, sister-taxa GLMs, and fit process based models in EvoRAG (see Box 1, 7-8 and
269 Supplementary Methods). We did not perform Mantel tests on the sister-taxa data because such
270 tests require complete matrices and distance matrices with data for only sister taxa would mostly
271 contain empty cells (i.e. all those cells that correspond to non sister taxa species pairs). We
272 compared the fit of process-based phenotypic models with and without species interactions
273 (Brownian motion, Ornstein-Uhlenbeck, diversity dependent, and matching competition models;
274 see Box 1, 5 and Supplementary Methods) to the full datasets from divergence scenarios using
275 the R packages geiger (Pennell et al. 2014) and RPANDA (Morlon et al. 2016). We acknowledge
276 that diversity-dependent models were not designed to analyze character displacement *per se*, but
277 because they incorporate interspecific interactions, we hypothesized that (and wanted to test if)
278 they could be useful in doing so. We did not apply process-based models to convergence
279 scenarios because the necessary model fitting tools have yet to be developed (see Discussion).
280 Our tests of predictors of species interactions involved assessing the significance of the
281 relationship between phenotypic similarity and species interactions (i.e., whether the species
282 interact where they occur in sympatry). Since the response variable is binary, we fit non-
283 phylogenetic logistic regressions, logistic PLMMs, and employed the simulation approach (see
284 Supplementary Methods). We did not perform Mantel tests or sister-taxa analyses because the
285 species pair matrix was incomplete (species that do not coexist cannot interact) and typically too
286 few sister taxa occurred in sympatry for regression analysis.
287
288
289 **RESULTS**
290
291 *Divergent Character Displacement*
292 When all possible pairwise comparisons are included in analyses, the ability of most
293 methods to detect divergent character displacement depends on the presence of the OU process.
294 As expected, non-phylogenetic regression analyses have a high Type I error rate in either
295 scenario (Figs. 2Ai,iv, S2Ai,iv [NB: throughout, results for low sympatric speciation
296 biogeographies are plotted in the main text and high sympatric speciation biogeographies in the
297 supplement]). When the OU process is present ($\psi = 2$), all methods generally have low Type I
298 error rates and high power (Figs. 2Aiv-vi, S2iv-vi, Supplementary Tables). However, when there

is no pull toward a peak ($\psi = 0$), the Type I error rate is higher for Mantel tests (Figs. 2Ai-ii, S2i-ii), and the power is much lower for all methods, though the pppMantel and raw Mantel perform better than the simulation and PLMM methods (Figs. 2Aiii, Fig. S2iii). Repulsion is easier to detect against an OU background of traits converging toward a common optimum than against a background of traits diverging under BM, likely because the repulsion process is more active when species occupy similar trait space (Figs. S3, S4). High rates of sympatric speciation and dispersal tend to slightly decrease the power of all methods (Fig. S2ii,iv, Supplementary Tables).

The ability to detect divergence was relatively similar for $m = 1$ and $m = 2$, but declined for $m = 10$ (Fig. S5). This is due to a positive relationship between the ability to detect character displacement and the ratio of ψ:m (Fig. S6), resulting from a higher absolute magnitude of repulsion when both processes are present (Figs. S4, S6), indicating that this ratio impacts the ability to detect divergence more than the raw value of m.

For sister-taxa analyses, there is a high probability of falsely concluding that character displacement occurred in datasets simulated under BM and, to a lesser extent, OU, whether analyzed with simple linear regressions, sister-taxa GLMs, or PLMMs (Figs. 2Bi,iii, S2Bi,iii). As with the whole-tree approach, the power tends to increase and Type I error rate tends to decrease in datasets with attraction toward a single-stationary peak (Figs. 2Biv-vi, S2Biv-vi). However, the overall power to infer the presence of divergence was low with sister-taxa analyses (Figs. 2Biii,vi, S2Biii,vi). Inferences were generally better when dispersal was high, which may reflect the elevated observed divergence in high dispersal scenarios (Fig. S3). Allopatric speciation scenarios increased the probability of Type I error (Fig. 2Bi-ii).

For the phylogenetic trait model-fitting analyses, BM and OU were generally correctly chosen when they were the generating models (i.e., when $m = 0$ and when $\psi = 0$ or 2, respectively, Figs. 3, S8). When $\psi = 0$ and $m > 0$, the matching competition (MC) model with biogeography is consistently the best-fit model (Figs. 3A, S8A). When $m > 0$ and $\psi = 2$, the diversity dependent exponential (DD_{exp}) model with biogeography was favored over other models in most scenarios (Figs. 3B, S8B), with positive rate parameters estimated in the maximum likelihood solution (Fig. S9). The biogeographic scenario did not greatly affect the outcome of model fitting, though correct models were slightly more supported when dispersal was high (Fig. S10), again in agreement with the observed magnitude of repulsion (Fig. S3). Although the models are less identifiable when $m = 10$ and $\psi = 2$ (Figs. 3, S8), this results from variation in the ψ:m ratio— there is a ratio of ψ:m around which these models cannot be distinguished (Fig. S11).

Process-based models fit to sister-taxa datasets in EvoRAG did not mistakenly identify an effect of species interactions when they were absent (Fig. S4A, C, Table 2), but they were unable to identify the effect of competition when $\psi = 0$ (Fig. S4B, Table 2). However, as with process-based models fit to the whole phylogeny, when data were simulated with both repulsion and a pull toward a stable peak, a model where evolutionary rates vary linearly with the number of sympatric taxa is often the best-fit model, though generally with only a marginally lower AICc value (i.e., ΔAICc < 2) than BM (Fig. S4, Table 2).

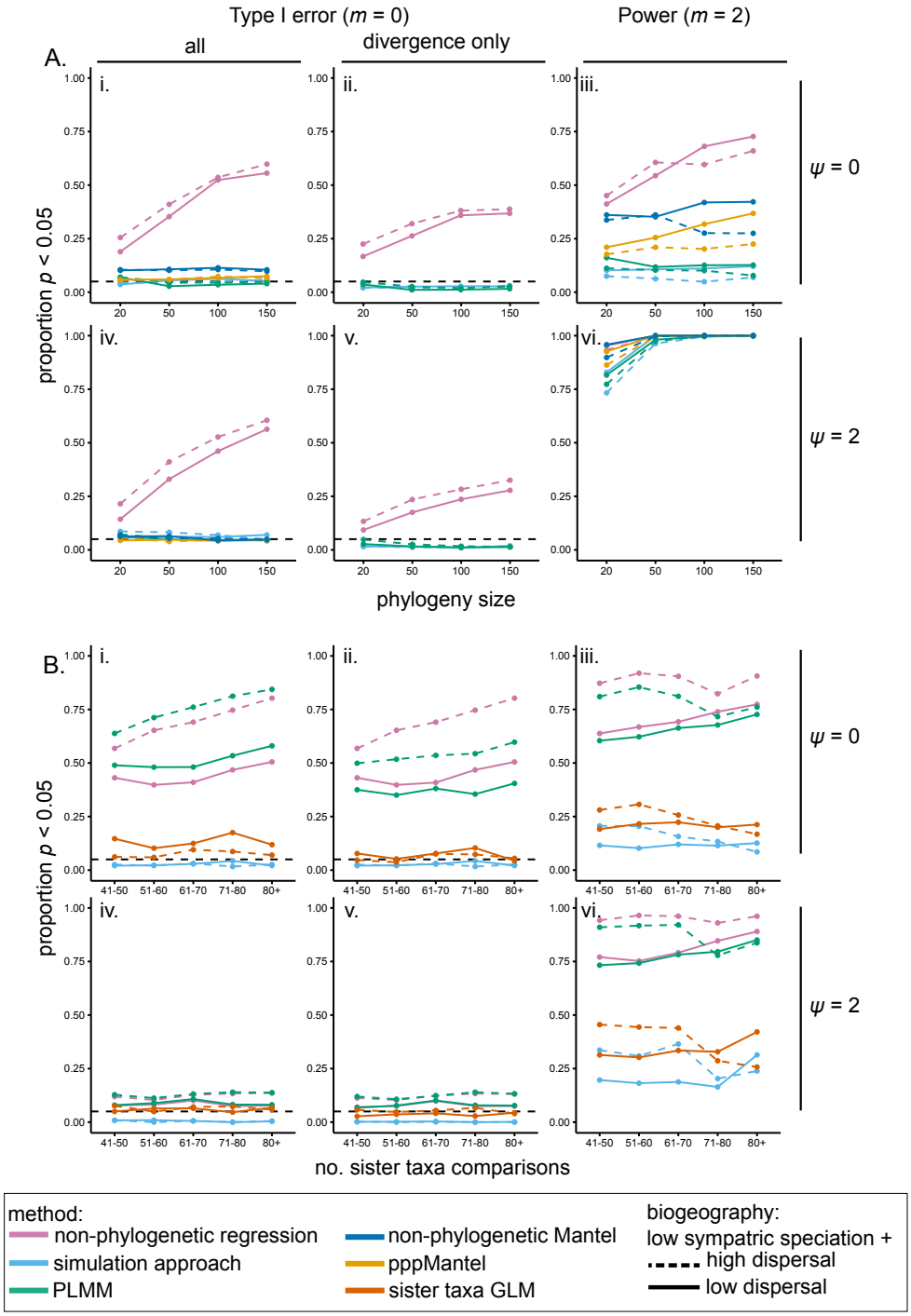

Figure 2. Proportion of statistically significant analyses in datasets simulated under divergent character displacement in biogeographic scenarios with low sympatric speciation rates. A. Results from approaches using data from all pairwise comparisons in a clade, plotted as a function of the phylogeny size and dispersal rate when i-ii. $m = 0$ and $\psi = 0$ (i. all analyses and ii. only analyses returning divergence in sympatry), iii. $m = 2$ and $\psi = 0$, iv-v. $m = 0$ and $\psi = 2$ (iv. all analyses and v. only analyses returning divergence in sympatry), and vi. $m = 2$ and $\psi = 2$. B. Results from analyses of sister-taxa culled from complete phylogenies binned by the number of resulting species pairs, plotted as a function of the number of sister taxa comparisons and

dispersal rate when i-ii. $m = 0$ and $\psi = 0$ (i. all analyses and ii. only analyses returning divergence in sympatry), iii. $m = 2$ and $\psi = 0$, iv-v. $m = 0$ and $\psi = 2$ (iv. all analyses and v. only analyses returning divergence in sympatry), and vi. $m = 2$ and $\psi = 2$. For scenarios where $m = 2$, only the proportion of significant results showing divergence are plotted. Dashed horizontal lines represent a Type I error rate of 5%.

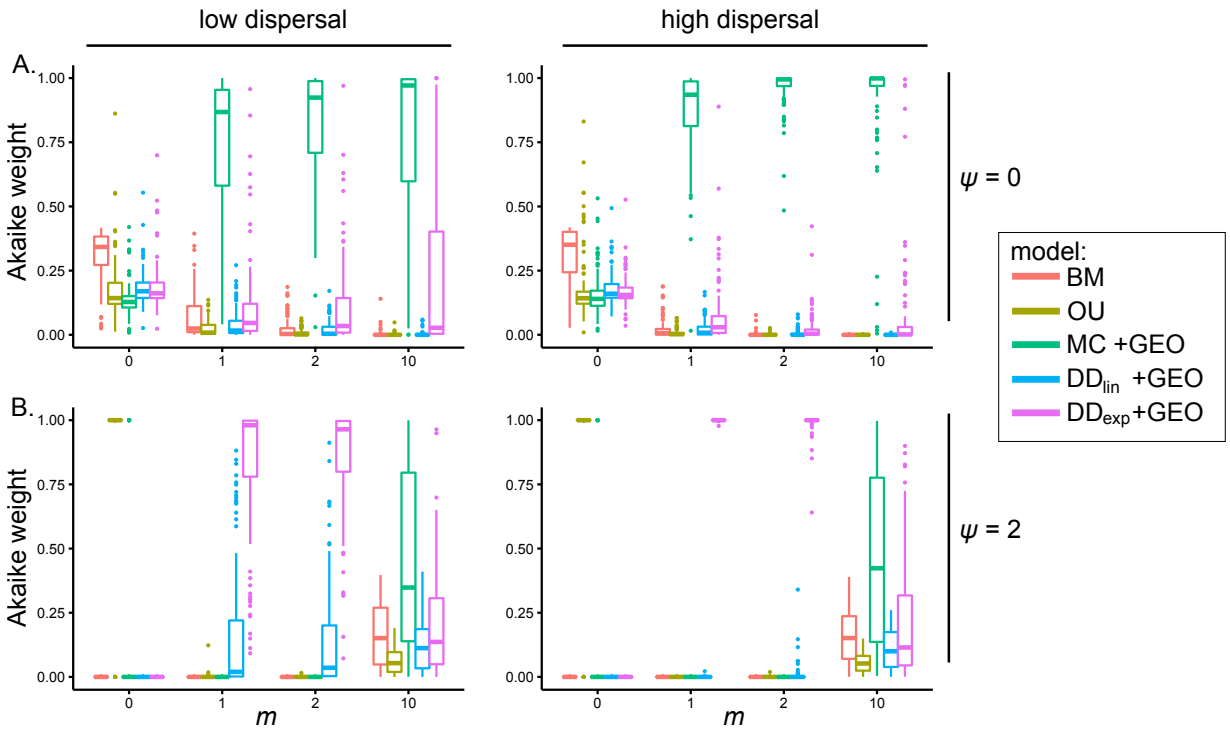

Figure 3. Boxplots of Akaike weights for each trait model fit to simulated datasets in biogeographic scenarios with low sympatric speciation rates as a function of *m* in trees with 100 species. A. When OU is absent, BM is the best-fit model when *m* = 0, and the matching competition model with biogeography is the best model when competitive divergence is present. B. When OU is present, OU is the best-fit model when *m* = 0, and the diversity-dependent exponential model with biogeography is the best model when competitive divergence is present and *ψ:m* is relatively high.

Convergent Character Displacement

As with divergent character displacement, with all pairwise species combinations, the ability of most methods to detect convergent character displacement depends on the presence of the OU process on the resource-use trait: datasets simulated under an OU model were more likely to be statistically significant (Figs. 4A.iv-vi, S12A.iv-vi) across all methods than those with BM simulated resource-use traits (Figs. 4A.i-iii, S12A.i-iii). Again, this is likely because the presence of the OU process in the resource-use trait amplifies the magnitude of convergence (Fig. S13, S14). Overall, however, only the simulation approach had substantial power (> 0.80) to detect convergent character displacement (Table 1), and only in trees with 100 or more tips and datasets with the OU process in the simulated resource-use trait. Indeed, the non-phylogenetic regressions often (spuriously) detected divergence rather than the simulated convergence, especially in smaller trees (Supplementary Tables). Both types of Mantel tests were unable to detect convergence, in fact having a higher Type I error rate (detecting divergence in BM simulated datasets, Supplementary Tables) than power. As with divergent character displacement, there was a tendency for higher power in lower dispersal scenarios.

The power to detect convergence generally increased with increasingly negative values of m, the maximum strength of attraction in the signal trait when species are identical in the resource-use trait (Fig. S15), though as m gets large, the probability that all species converge on the same trait value increases, especially when $\psi_{\text{resource}} = 2$ (data not shown).

Regardless of whether resource-use traits are simulated under OU or BM, when there is no convergence, most methods used for sister-taxa analyses tend to have high Type I error rates, though these analyses return an erroneous inference of divergence, rather than convergence, between sister taxa (Figs. 4B.i,ii,iv,v, S12B.i,ii,iv,v, Supplementary Tables). Sister-taxa analyses had overall low power to detect convergence when it did exist, and non-phylogenetic regressions often detected divergence, rather than convergence (Supplementary Tables). When convergence was detected, it tended to be in biogeographic scenarios with high dispersal, likely reflecting the overall magnitude of convergence achieved (Fig. S13). As with divergent character displacement simulations, the allopatric speciation biogeographic scenarios were more likely to lead to higher Type I error rates (Figs. 4B.i,iv). Process-based models fit to sister-taxa datasets in EvoRAG did not erroneously detect divergence or convergence (i.e., BM was the best-fit model when $m = 0$, Fig. S14 A, C, Table 2), but they could not detect an effect of species interactions when convergence was present, at least for the number of sister taxa in this study, as OU was the best-fit model when $m = -0.25$ (Fig. S14 B, C, Table 2).

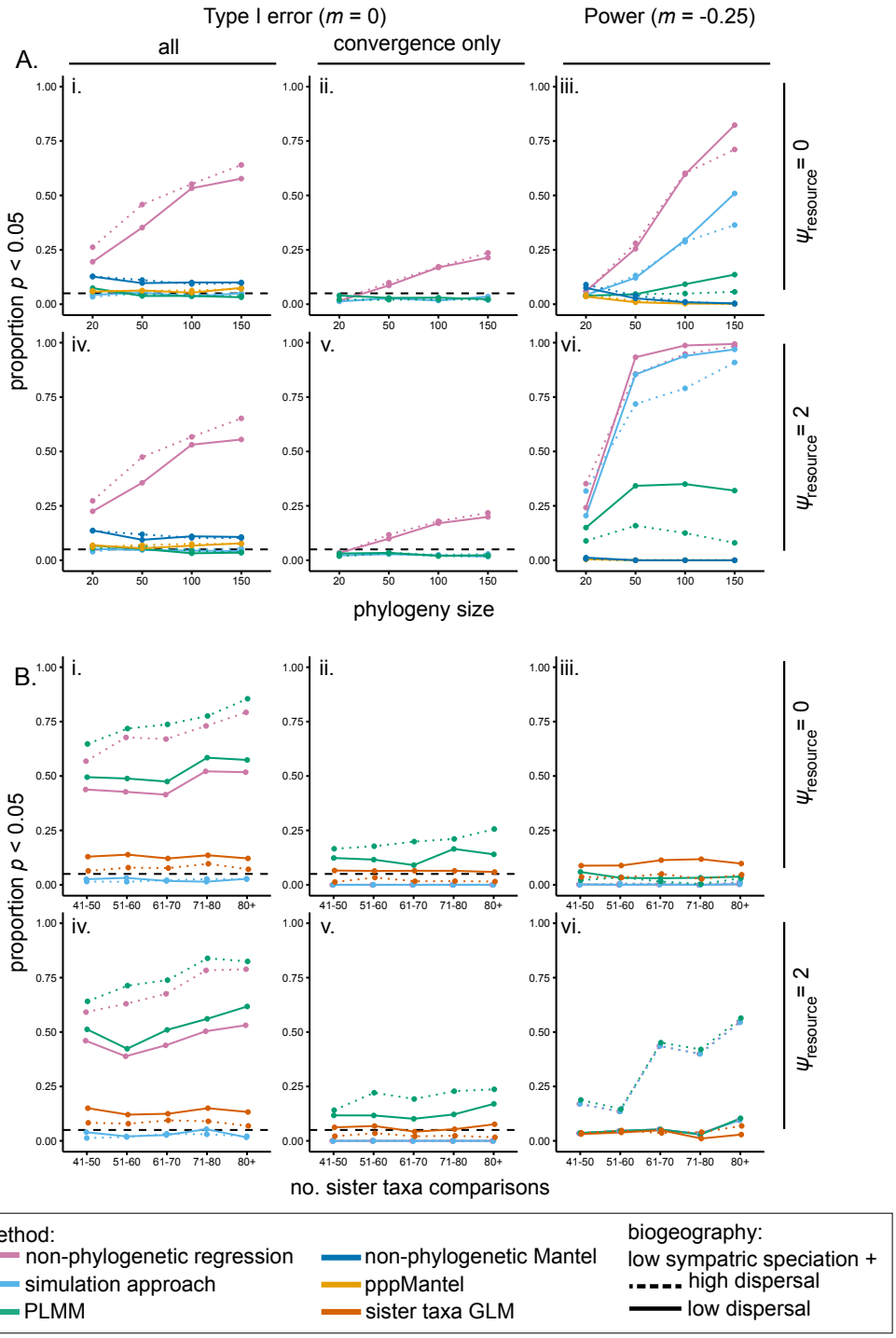

Figure 4. Proportion of statistically significant analyses in datasets simulated under convergent character displacement in biogeographic scenarios with low sympatric speciation rates. A. Results from approaches using data from all pairwise comparisons in a clade, plotted as a function of the phylogeny size and dispersal rate when i-ii. $m = 0$ and $\psi_{resource} = 0$ (i. all analyses and ii. only analyses returning convergence in sympatry), iii. $m = -0.25$ and $\psi_{resource} = 0$, iv-v. $m = 0$ and $\psi_{resource} = 2$ (iv. all analyses and v. only analyses returning convergence in sympatry), and vi. $m = -0.25$ and $\psi_{resource} = 2$. B. Results from analyses of sister-taxa culled from complete

phylogenies binned by the number of resulting species pairs, plotted as a function of the number of sister taxa comparisons and dispersal rate when i-ii. $m = 0$ and $\psi_{resource} = 0$ (i. all analyses and ii. only analyses returning convergence in sympatry), iii. $m = -0.25$ and $\psi_{resource} = 0$, iv-v. $m = 0$ and $\psi_{resource} = 2$ (iv. all analyses and v. only analyses returning convergence in sympatry), and vi. $m = -0.25$ and $\psi_{resource} = 2$. For scenarios where $m = -0.25$, only the proportion of significant results showing convergence are plotted. Dashed horizontal lines represent a Type I error rate of 5%.

Predicting Interspecific Interactions

Although all three methods used to identify traits that are causally related to interspecific interactions had high power (>>0.8, Table 1, Supplementary Tables) to do so in the parameter space explored here (Figs. 5ii,iv, S16ii,iv), only the simulation approach had both high power and a low Type I error rate (Table 1), whereas non-phylogenetic regressions and PLMMs had fairly high Type I error rates (Table 1) when interactions were simulated based on similarity in a trait other than the measured one (Fig. 5i,iii, S16i,iii). The power to detect an interaction was not greatly affected by the coefficients used to simulate datasets (Fig. S17). Biogeography did not have a large impact on analyses, though there were slightly higher Type I error in low dispersal scenarios (Fig. 5i,iii).

DISCUSSION

As open-access databases with species range, trait, and phylogenetic data rapidly expand, investigators are able to test hypotheses about the relationships between interspecific interactions and phenotypic evolution at an unprecedented scale. Understanding the relative strengths and weaknesses of phylogenetic comparative methods available for testing such hypotheses is thus paramount. We found that currently used methods for detecting causal relationships between interspecific interactions and species phenotypes suffer from severe limitations (Tables 1,2).

Overall, standard methods are better at detecting divergent character displacement when divergence does not drive unbounded trait evolution (i.e., when selection acts against extreme phenotypes). Consistent with previous reports (Harmon and Glor 2010; Guillot and Rousset 2013), Mantel tests had high Type I error rates and both standard and pppMantel tests have low power (Table 1, Figs. 2Ai, S2Ai). Alarmingly, we found that commonly used sister taxa approaches have high Type I error rates (Table 2, Figs. 2Bi,iv, S2Bi,iv, 4Bi,iv, S12Bi,iv, Supplementary Tables), which would lead investigators to conclude that divergent character displacement had acted when, in fact, it had not, and none have a reasonable combination of Type I error and power.

Fitting process-based phylogenetic trait models to datasets simulated with divergent character displacement yielded more consistent patterns (Fig. 3). Without attraction toward a single stationary peak to bound trait evolution, the matching competition (MC) model with biogeography was predominantly the best-fit model. For datasets simulated with the OU process, the diversity-dependent exponential (DD_{exp}, see Box 1) model with biogeography was the best-fit model, and similarly a model with a linear relationship between evolutionary rates and the number of sympatric taxa often fit sister-taxa datasets, though with much lower power overall

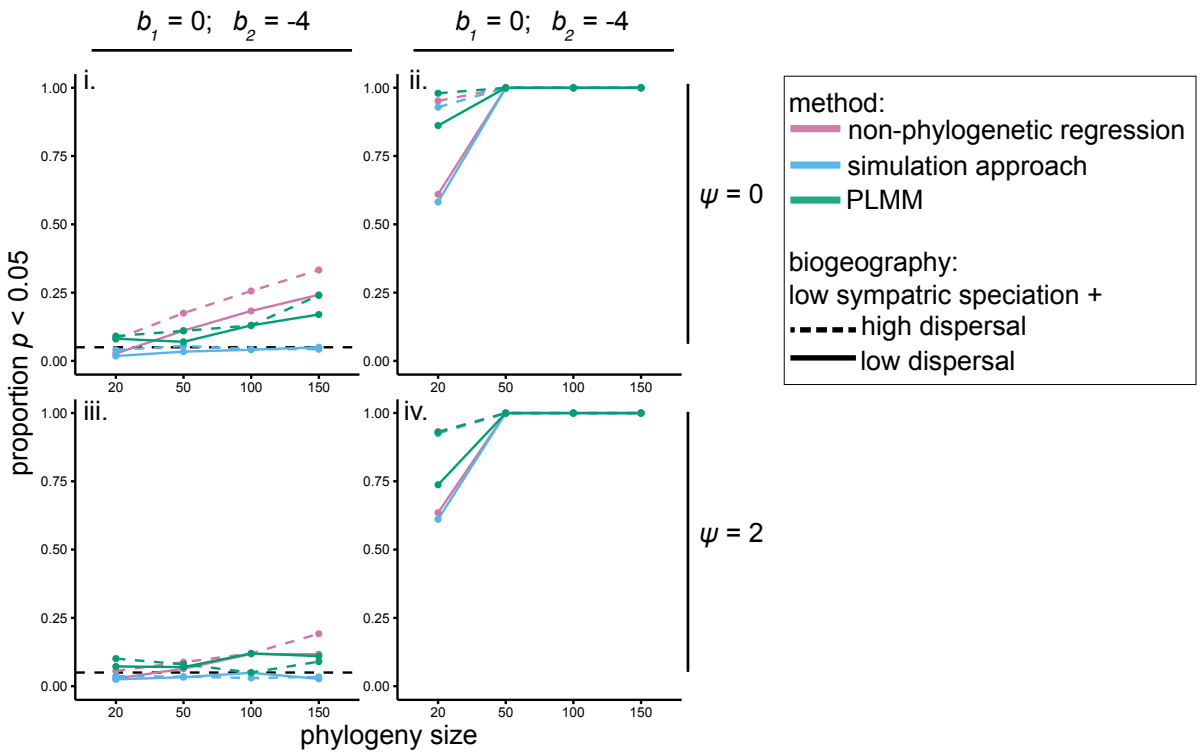

Figure 5. Proportion of statistically significant analyses in datasets with interactions simulated under a simple phenotype matching process in biogeographic scenarios with low sympatric speciation rates. Results from analyses where the measured trait was simulated under BM (i, ii) or OU (iii, iv), plotted as a function of the phylogeny size and dispersal rate when i. b_1 (the simulation coefficient determining the relationship between the interaction and the measured trait) = 0, b_2 (the simulation coefficient for an unmeasured trait) = -4, and ψ = 2, ii. b_1 = -4, b_2 = 0, and ψ = 2, iii. b_1 = 0, b_2 = -4, and ψ = 0, and iv. b_1 = -4, b_2 = 0, and ψ = 0.

463 **Table 1.** Summary of the statistical properties of the analytical approaches tested under scenarios using data from all tips (i.e., with
464 sister-taxa analyses excluded). Values refer to the range of type I error rates and power levels for each tree size ≥50, averaged across
465 biogeographic scenarios and scenarios where ψ or ψ_{nf} = 0 or 2. Power refers to only those statistically significant tests in the
466 appropriate tail (i.e., in the lower tail for divergent character displacement and upper tail for convergent character displacement). For
467 each analytical scenario, the cell with the method with the best trade-off between Type I error and power is highlighted.
468

Analysis	**non-phylogenetic regression**		**Mantel test**		**pppMantel test**		**PLMM**		**simulation test**		**process-based models**	
	type I	*power*	*type I*	*power*	*type I*	*power*	*type I*	*power*	*type I*	*power*	*type I**	*power*[†]
divergent char. displacement	0.37-0.61	0.51-1	0.05-0.10	0.29-1	0.04-0.06	0.19-1	0.05-0.06	0.12-1	0.05-0.07	0.08-1	0.04-0.05	0.91-0.94
convergent char. displacement	0.40-0.60	0.31-0.99	0.08-0.09	0-0.02	0.05-0.06	0-0.01	0.05-0.07	0.07-0.26	0.04-0.05	0.12-0.91	--	--
predicting spp. interactions	0.08-0.3	1	--	--	--	--	0.07-18	1	0.03-0.04	1	--	--

469 *Type I error rate calculated as the proportion of datasets simulated without divergence for which a model that includes species interaction— DD_{exp}, DD_{lin}, or MC—was chosen by
470 model selection (i.e., for which ΔAICc = 0 and ΔAICc for all other models > 2).
471 [†] Power calculated as the proportion of datasets simulated with divergence for which either DD_{exp}, DD_{lin}, or MC was chosen by model selection.
472
473

Table 2. Summary of the statistical properties of the analytical approaches tested under scenarios using sister-taxa analyses. Values refer to the range of type I error rates and power levels, averaged across biogeographic scenarios and scenarios where ψ or ψ_{nf} = 0 or 2. Power refers to only those statistically significant tests in the appropriate tail (i.e., in the upper tail for divergent character displacement and lower tail for convergent character displacement). We caution against using sister-taxa approaches to test for character displacement.

Analysis	**non-phylogenetic regression**		**sister-taxa GLM**		**PLMM**		**simulation test**		**process-based models in EvoRAG**	
	type I	*power*	*type I*	*power*	*type I*	*power*	*type I*	*power*	*type I**	*power*[†]
divergent char. displacement	0.07-0.42	0.68-0.75	0.05-0.07	0.20-0.34	0.08-0.50	0.70-0.78	0.01-0.02	0.18-0.31	0.04-0.07	0.03-0.36
convergent char. displacement	0.33-0.43	0.01-0.2	0.07	0.04-0.06	0.41-0.5	0.02-0.21	0.03	0.01-0.2	0.04	0.09-0.55

*Type I error rate calculated as the proportion of datasets simulated without divergence for which a model that includes a linear dependency on the number of sympatric lineages—BM_{linear} or OU_{linear_beta}—was chosen by model selection (i.e., for which ΔAICc = 0 and ΔAICc for all other models > 2).

[†] Power calculated as the proportion of datasets simulated with divergence for which either BM_{linear} or OU_{linear_beta} was chosen by model selection.

485 (Fig S4, Table 2). In the DD_{exp} model, rates of trait evolution vary exponentially with the
486 number of sympatric lineages through time, so incorporating the effect of interspecific
487 interactions on the rate of trait of evolution but not explicitly modeling the process of character
488 displacement acting on the mean trait values. It may nonetheless provide a useful proxy for
489 detecting patterns that are similar to those left by character displacement, in the absence of a
490 process-based model that incorporates both attraction toward an optimum trait value and
491 divergent character displacement. We emphasize, however, that statistical support for the DD_{exp}
492 model does not in itself constitute decisive evidence that character displacement has occurred, as
493 other processes may generate increasing evolutionary rates with increasing lineage diversity.
494 Given that the DD_{exp} model is the best-fit model in parameter space where other methods also
495 perform well, combined evidence from model-fitting and other, non-process based methods
496 would constitute a strong case for the presence of character displacement. In the absence of tip
497 data (e.g., due to incomplete sampling or traits that are inherently measured as pairwise
498 properties), process-based models are unsuitable and we recommend using data from as many
499 species pairs as possible—not just sister taxa—and using simulation approaches or PLMMs.
500 Interestingly, even though most previous investigators have used the DD_{exp} model to
501 represent a decline in ecological opportunity with increasing species richness (Mahler et al.
502 2010; Weir and Mursleen 2013), the maximum likelihood estimates of the rate parameters for
503 this model were positive, rather than negative, when both divergence and the OU process were
504 present (Fig. S9). This is consistent with our finding of increasing evolutionary rates with
505 increasing species richness (Figs. S3, S4, S7) in this scenario. An increase in the rate of
506 evolutionary changes in trait values toward the present likely results from selection not only
507 restricting species to certain trait space but also partitioning that space. The resulting adaptive
508 landscape is therefore rapidly changing, causing accelerating evolutionary rates as lineages fill
509 this increasingly constrained space.
510 The MC model (Box 1) is similar to the model used to simulate data (Eq. 1), with the
511 assumption that α is very small ($<< 1$) and consequently, competitive interactions are affected by
512 the mean trait values of all sympatric species, rather than by pairwise similarity (Nuismer and
513 Harmon 2015; Drury et al. 2016). Biologists, however, generally assume that competition is
514 stronger between phenotypically similar species (Brown and Wilson 1956). Our results show that
515 this assumption does not render the MC model useless for studying character displacement, as
516 the MC model is the best-fit model for many datasets simulated under the character displacement
517 model used here. Nevertheless, the finding that the DD_{exp} model is the best-fit model in datasets
518 simulated with the OU process indicates that the MC model is not a perfect model of character
519 displacement.
520 For datasets simulated including the OU process, the ratio of the pull-parameter in the
521 OU portion of the model to the maximum amount of repulsion (ψ:m) had a consistent impact
522 across all methods, which results from the overall larger magnitude of evolutionary changes in
523 traits in scenarios with a high ψ:m ratio (Figs. S3, S4, S7). As ψ:m approached 1, all methods
524 were better at detecting character displacement. Currently, there are no analytical approaches that
525 can disentangle the simultaneous impact of attraction toward a peak and divergence due to
526 competition, though we hope our results will inspire development of such tools.
527 Unlike for divergent character displacement, available statistical methods for detecting
528 convergence in comparative datasets generally do a poor job of detecting convergence, with the
529 simulation method outperforming others (Table 1). With whole-dataset approaches, Type I error
530 rates are acceptable for phylogenetic analyses (~5%), however, so although detecting

convergence is difficult, the risk of mistakenly detecting convergence is low. In sister-taxa analyses, although Type I error rates are high for PLMMs (Table 2), these largely return erroneous divergence results, rather than erroneous convergence (Figs. 4Bii,v, S12Bii,v). In short, if an empiricist detects convergence in their dataset, they can be fairly confident in the result. Currently, there are no tools to fit phylogenetic trait models of convergence between species (e.g., Nuismer & Harmon 2015); such tools might more successfully identify convergent character displacement in comparative datasets than the available statistical methods.

For both divergent and convergent character displacement scenarios, we found that sister-taxa GLMs and the simulation approach had a mean Type I error rate near 5% (Table 2). However, in some scenarios, the Type I error for sister taxa GLMs was much higher than for the simulation approach (Figs. 2Bi, 4Bi, Supplementary Tables), which suggests that including a model-based estimate of the rate of trait evolution more properly accounts for the effect of divergence than simply including the branch lengths separating sister taxa as a covariate in analyses to control for variation in the amount of time sister taxa have had to diverge from one another. The high overall Type I error rate for sister-taxa analyses may also result from the unrealistic assumption that transitions between allopatry and sympatry are uncommon along branches connecting sister taxa (Weir and Price 2011; Tobias et al. 2014). Supporting this explanation, we found that biogeographic scenarios with high levels of sympatric speciation and low dispersal tended to have overall lower Type I error rates (cf. Figs. 2,S2; Figs. 4,S12).

The outlook for identifying which traits drive species interaction is brighter. The statistical methods available to test for causal relationships between phenotypic similarity and interactions between species have very high power. The simulation approach has a low Type I error rate when causal relationships are simulated based on an unmeasured trait, although non-phylogenetic regressions and PLMMs suffer from relatively high Type I error rates. While we did not simulate interactions between clades, our results are likely applicable to other empirical questions, such as identifying traits that predict links in ecological networks (Rafferty and Ives 2013; Hadfield et al. 2014; Eklöf and Stouffer 2016).

By simulating datasets with various types of interactions between species across different modes of speciation and dispersal rates, we have shown that many of the methods that investigators use to analyze empirical datasets have low power to detect such patterns (Table 1). Worse still, widely-used sister taxa approaches, including standard regressions and sister-taxa GLMs, often detected character displacement in datasets that were simulated under a simple BM model (Figs. 2Bi-ii, 4Bi-ii). We therefore urge investigators to use caution when interpreting the results of such analyses. When process-based models could be fit to these datasets, they tended to consistently identify patterns of divergence (i.e., either the matching competition model or a diversity-dependent model is the best fit model >91% of the time). Thus, when possible, empiricists should employ such methods. Statistical tools to fit process-based models of phenotypic evolution including species interactions are in their infancy (Drury et al. 2016) and many possible models are not yet available (e.g., convergent character displacement, character divergence in the presence of an adaptive pull towards a peak). We hope that our results encourage the continued development of such tools.

In closing, we note that divergent character displacement is erroneously detected with many statistical approaches, indicating that there may be an overrepresentation of empirical studies that imply that divergence has occurred. Conversely, convergent character displacement is often hard to detect with existing methods, suggesting that convergence in signal traits (e.g.,

Cody 1969, 1973; Tobias et al. 2014; Losin et al. 2016) might be more prevalent than previously thought.

ACKNOWLEDGEMENTS

This research was funded by the European Research Council (grant 616419-PANDA to HM) and the National Science Foundation (grant DEB-1457844 to GFG). We thank M. Manceau, J. Clavel, E. Lewitus, O. Maliet, and O. Missa for feedback.

584 **REFERENCES**

585 Allen W.L., Stevens M., Higham J.P. 2014. Character displacement of Cercopithecini primate
586 visual signals. Nat. Commun. 5:4266.
587 Bacquet P.M.B., Brattström O., Wang H.L., Allen C.E., Löfstedt C., Brakefield P.M.,
588 Nieberding C.M. 2015. Selection on male sex pheromone composition contributes to
589 butterfly reproductive isolation. Proc. R. Soc. London B Biol. Sci. 282:20142734.
590 Brown W.L., Wilson E.O. 1956. Character displacement. Syst. Zool. 5:49–64.
591 Cadotte M., Albert C.H., Walker S.C. 2013. The ecology of differences: Assessing community
592 assembly with trait and evolutionary distances. Ecol. Lett. 16:1234–1244.
593 Cavender-Bares J., Kozak K.H., Fine P.V.A., Kembel S.W. 2009. The merging of community
594 ecology and phylogenetic biology. Ecol. Lett. 12:693–715.
595 Cody M.L. 1969. Convergent characteristics in sympatric species: a possible relation to
596 interspecific competition and aggression. Condor. 71:223–239.
597 Cody M.L. 1973. Character Convergence. Annu. Rev. Ecol. Syst. 4:189–211.
598 Davies J.T., Meiri S., Barraclough T.G., Gittleman J.L. 2007. Species co-existence and character
599 divergence across carnivores. Ecol. Lett. 10:146–152.
600 Drury J.P., Clavel J., Manceau M., Morlon H. 2016. Estimating the effect of competition on trait
601 evolution using maximum likelihood inference. Syst. Biol. 65:700–710.
602 Drury J.P., Okamoto K.W., Anderson C.N., Grether G.F. 2015. Reproductive interference
603 explains persistence of aggression between species. Proc. R. Soc. B. 282:20142256.
604 Eklöf A., Stouffer D.B. 2016. The phylogenetic component of food web structure and intervality.
605 Theor. Ecol. 9:107–115.
606 Elias M., Gompert Z., Jiggins C., Willmott K. 2008. Mutualistic interactions drive ecological
607 niche convergence in a diverse butterfly community. PLoS Biol. 6:e300.
608 Felsenstein J. 1985. Phylogenies and the comparative method. Am. Nat. 125:1–15.
609 Garland T., Dickerman A.W., Janis C.M., Jones J.A. 1993. Phylogenetic analysis of covariance
610 by computer simulation. Syst. Biol. 42:265–292.
611 Grant P.R. 1972. Convergent and divergent character displacement. Biol. J. Linn. Soc. 4:39–68.
612 Grant P.R., Grant B.R. 2011. How and Why Species Multiply: the Radiation of Darwin's
613 Finches. Princeton, NJ: Princeton University Press.
614 Grant P.R., Grant B.R. 2006. Evolution of character displacement in Darwin's finches. Science
615 313:224–226.
616 Grether G.F., Anderson C.N., Drury J.P., Kirschel A.N.G., Losin N., Okamoto K., Peiman K.S.
617 2013. The evolutionary consequences of interspecific aggression. Ann. N. Y. Acad. Sci.
618 1289:48–68.
619 Grether G.F., Losin N., Anderson C.N., Okamoto K. 2009. The role of interspecific interference
620 competition in character displacement and the evolution of competitor recognition. Biol.
621 Rev. 84:617–635.
622 Guillot G., Rousset F. 2013. Dismantling the Mantel tests. Methods Ecol. Evol. 4:336–344.
623 Hadfield J.D., Krasnov B.R., Poulin R., Nakagawa S. 2014. A tale of two phylogenies:
624 comparative analyses of ecological interactions. Am. Nat. 183:174–187.
625 Hadfield J.D., Nakagawa S. 2010. General quantitative genetic methods for comparative biology:
626 phylogenies, taxonomies and multi-trait models for continuous and categorical characters. J.
627 Evol. Biol. 23:494–508.
628 Hansen T.F., Martins E.P. 1996. Translating between microevolutionary process and
629 macroevolutionary patterns: The correlation structure of interspecific data. Evolution.

50:1404–1417.
Harmon L.J., Glor R.E. 2010. Poor statistical performance of the Mantel test in phylogenetic comparative analyses. Evolution 64:2173–2178.
Harmon L.J., Losos J.B., Jonathan Davies T., Gillespie R.G., Gittleman J.L., Bryan Jennings W., Kozak K.H., McPeek M.A., Moreno-Roark F., Near T.J., Purvis A., Ricklefs R.E., Schluter D., Schulte J.A., Seehausen O., Sidlauskas B.L., Torres-Carvajal O., Weir J.T., Mooers A.T. 2010. Early bursts of body size and shape evolution are rare in comparative data. Evolution 64:2385–2396.
Hilbe J.M. 2009. Logistic regression models. CRC press.
Lapointe F.J., Garland T. 2001. A generalized permutation model for the analysis of cross-species data. J. Classif. 18:109–127.
Losin N., Drury J.P., Peiman K.S., Storch C., Grether G.F. 2016. The ecological and evolutionary stability of interspecific territoriality. Ecol. Lett. 19:260–267.
Mahler D.L., Revell L.J., Glor R.E., Losos J.B. 2010. Ecological opportunity and the rate of morphological evolution in the diversification of greater Antillean anoles. Evolution 64:2731–2745.
Mantel N. 1967. The detection of disease clustering and a generalized regression approach. Cancer Res. 27:209–220.
Martin P.R., Montgomerie R., Lougheed S.C. 2010. Rapid sympatry explains greater color pattern divergence in high latitude birds. Evolution 64:336–347.
Martins E.P., Garland Jr T. 1991. Phylogenetic analyses of the correlated evolution of continuous characters: a simulation study. Evolution 45:534–557.
Matzke N.J. 2014. Model selection in historical biogeography reveals that founder-event speciation is a crucial process in island clades. Syst. Biol. 63:951–970.
Medina-García A., Araya-Salas M., Wright T.F. 2015. Does vocal learning accelerate acoustic diversification? Evolution of contact calls in Neotropical parrots. J. Evol. Biol. 28:1782–1792.
Morlon H., Lewitus E., Condamine F.L., Manceau M., Clavel J., Drury J. 2016. RPANDA: an R package for macroevolutionary analyses on phylogenetic trees. Methods Ecol. Evol. 7:589–597.
Nuismer S.L., Harmon L.J. 2015. Predicting rates of interspecific interaction from phylogenetic trees. Ecol. Lett. 18:17–27.
Pennell M.W., Eastman J.M., Slater G.J., Brown J.W., Uyeda J.C., FitzJohn R.G., Alfaro M.E., Harmon L.J. 2014. geiger v2. 0: an expanded suite of methods for fitting macroevolutionary models to phylogenetic trees. Bioinformatics.:btu181.
Pfennig K.S., Pfennig D.W. 2009. Character displacement: Ecological and reproductive responses to a common evolutionary problem. Q. Rev. Biol. 84:253–276.
Pigot A.L., Tobias J.A. 2014. Dispersal and the transition to sympatry in vertebrates. Proc. R. Soc. B Biol. Sci. 282:20141929.
Rafferty N.E., Ives A.R. 2013. Phylogenetic trait-based analyses of ecological networks. Ecology. 94:2321–2333.
Ree R.H., Smith S.A. 2008. Maximum likelihood inference of geographic range evolution by dispersal, local extinction, and cladogenesis. Syst. Biol. 57:4–14.
Rezende E.L., Diniz-Filho J.A.F. 2012. Phylogenetic analyses: Comparing species to infer adaptations and physiological mechanisms. Compr. Physiol. 2:639–674.
Rezende E.L., Lavabre J.E., Guimaraes Jr. P.R., Jordano P., Bascompte J. 2007. Non-random

coextinctions in phylogenetically structured mutualistic networks. Nature. 448:925-U6.
Roncal J., Henderson A., Borchsenius F., Cardoso S.R.S., Balslev H. 2012. Can phylogenetic signal, character displacement, or random phenotypic drift explain the morphological variation in the genus Geonoma (Arecaceae)? Biol. J. Linn. Soc. 106:528–539.
Schluter D. 2000. The Ecology of Adaptive Radiation. Oxford, UK: Oxford University Press.
Seddon N., Botero C.A., Tobias J.A., Dunn P.O., Macgregor H.E., Rubenstein D.R., Uy J.A., Weir J.T., Whittingham L.A., Safran R.J. 2013. Sexual selection accelerates signal evolution during speciation in birds. Proc. R. Soc. B Biol. Sci. 280:20131065.
Tobias J.A., Cornwallis C.K., Derryberry E.P., Claramunt S., Brumfield R.T., Seddon N. 2014. Species coexistence and the dynamics of phenotypic evolution in adaptive radiation. Nature. 506:359–363.
de Villemereuil P., Nakagawa S. 2014. General quantitative genetic methods for comparative biology. Modern Phylogenetic Comparative Methods and Their Application in Evolutionary Biology. Springer. p. 287–303.
Webb C.O., Ackerly D.D., McPeek M.A., Donoghue M.J. 2002. Phylogenies and community ecology. Annu. Rev. Ecol. Syst.:475–505.
Weber M.G., Mitko L., Eltz T., Ramírez S.R. 2016. Macroevolution of perfume signalling in orchid bees. Ecol. Lett.
Weir J.T., Lawson A. 2015. Evolutionary rates across gradients. Methods Ecol. Evol. 6:1278–1286.
Weir J.T., Mursleen S. 2013. Diversity-dependent cladogenesis and trait evolution in the adaptive radiation of the auks (Aves: Alcidae). Evolution. 67:403–416.
Weir J.T., Price T.D. 2011. Limits to speciation inferred from times to secondary sympatry and ages of hybridizing species along a latitudinal gradient. Am. Nat. 177:462–469.
Weir J.T., Wheatcroft D. 2011. A latitudinal gradient in rates of evolution of avian syllable diversity and song length. Proc. R. Soc. B Biol. Sci. 278:1713–20.
Willis P.M., Symula R.E., Lovette I.J. 2014. Ecology, song similarity and phylogeny predict natural hybridization in an avian family. Evol. Ecol. 28:299–322.

706 **Box 1. Methods for assessing the interplay between interspecific interactions and species**
707 **phenotypes**
708
709 Comparative analyses of the interplay between interspecific interactions and species
710 phenotypes can either be conducted on entire clades, or, commonly, on sister taxa—species pairs
711 that share a most recent common ancestor—that are culled from larger phylogenies. Such
712 analyses generally consist of testing the statistical significance of correlations between either
713 phenotypic similarity and geographic overlap (to test for divergent or convergent character
714 displacement) or species interactions and phenotypic similarity (to find predictors of species
715 interactions). As we are looking for correlations between pairwise comparisons (e.g., trait
716 similarity, biogeographical overlap, hybridization, magnitude of pre-zygotic isolation), rather
717 than "tip values" belonging to a single species, phylogenetically independent contrasts and
718 extensions of PGLS analyses (Felsenstein 1985; Rezende and Diniz-Filho 2012) cannot be used,
719 and alternative tests have been developed.
720
721 *1. Non-phylogenetic regressions*
722 "Non-phylogenetic regressions" refers to Generalized Linear Models (GLMs) that ignore
723 phylogenetic structure. Though less commonly applied to whole-clade analyses, investigators
724 sometimes use non-phylogenetic regressions for sister-taxa analyses, on the basis that branches
725 connecting sister taxa represent independent evolutionary histories (Felsenstein 1985).
726
727 *2. Mantel tests*
728 Several previous investigators have implemented Mantel tests (Mantel 1967) in analyses
729 of species-pair comparisons (e.g., Roncal *et al.* 2012). These tests are designed to assess
730 correlations between matrices, which here comprise interspecific trait distances or differences.
731 Existing accounts of Mantel tests describe procedures only for complete matrices, so they cannot
732 be used in many cases, including sister-taxa analyses (for which most off-diagonal elements of
733 distances matrices are by definition excluded) and in identifying predictors of species
734 interactions (e.g., hybridization), as only sympatric lineages can interact and setting values for
735 allopatric comparisons to zero would not make biological sense.
736
737 *3. Phylogenetically permuted partial Mantel tests*
738 Phylogenetically-permuted partial Mantel (pppMantel) tests (Lapointe and Garland 2001)
739 account for phylogenetic non-independence by permuting null datasets that are structured
740 phylogenetically, and are popular among investigators studying species interactions (e.g., Allen
741 *et al.* 2014; Willis *et al.* 2014; Medina-García *et al.* 2015). Like Mantel tests, pppMantel tests
742 also require complete interaction matrices.
743
744 *4. Phylogenetic linear mixed models*
745 In recent years, researchers have adapted animal models from quantitative genetics to
746 incorporate phylogenies as random effects in mixed-effect regressions on comparative datasets
747 (Hadfield & Nakagawa 2010). Such phylogenetic linear mixed models (PLMMs) have been
748 modified to accommodate pairwise species data (Tobias et al. 2014), wherein the identity of the
749 species being compared and the node connecting them in the phylogeny are included as random
750 effects. PLMMs are promising new tools, as they are not limited to sister-taxa data and model
751 predictions can be generated and plotted.

752
753 *5. Phylogenetic simulations*
754 Simulation approaches are widely used to control for phylogenetic non-independence in
755 tip data (Martins & Garland Jr 1991; Garland *et al.* 1993), and have been applied to pairwise
756 species comparisons (Elias et al. 2008; Drury et al. 2015; Losin et al. 2016). In these approaches,
757 trait evolution is simulated along phylogenies, often scaled such that the simulated tip data
758 resemble real data. Pairwise comparisons are then calculated on many simulated datasets and
759 used to generate a phylogenetically informed null distribution of test statistics against which to
760 compare test statistics calculated from the real data.
761
762 *6. Process-based models of phenotypic evolution*
763 In the statistical approaches outlined thus far, the data analyzed are measurements of
764 pairwise differences between species, and the statistical tests for the effect of species interactions
765 on trait evolution consist of testing for significant correlations between either phenotypic
766 similarity and geographic overlap or species interactions and trait similarity. However, it is also
767 possible to detect a signature of interspecific competition in the distributions of continuous trait
768 values across the tips of a phylogeny by fitting process-based models of phenotypic evolution to
769 the data. These models allow testing hypotheses about which processes are most likely to have
770 generated the observed distribution of traits in a clade (Hansen & Martins 1996).
771 Interspecific interactions have recently been incorporated into such models in two ways.
772 First, in diversity-dependent (DD) models, evolutionary rates change as a function (either linear
773 [DD_{lin}] or exponential [DD_{exp}]) of the number of extant lineages through time (e.g., Weir &
774 Mursleen 2013). Secondly, in the 'matching competition' (MC) model, trait evolution in an
775 evolving lineage varies as a function of the values of traits in other evolving lineages (Nuismer &
776 Harmon 2015, Drury *et al*. 2016). Comparing the fit of these models to other models that exclude
777 interspecific interactions (e.g., Brownian motion and Ornstein-Uhlenbeck models) tests whether
778 there is evidence that interspecific interactions have influenced the trajectory of trait evolution in
779 a clade.
780
781 *7. Sister-taxa GLMs*
782 If allopatric speciation is common, then sympatry occurs after a period of initial isolation,
783 resulting in a pattern where sympatric sister taxa are older than allopatric sister taxa. Thus, even
784 random genetic drift can generate a pattern in which sympatric lineages have more divergent
785 traits compared to allopatric lineages, simply because divergence has had more time to evolve
786 (Weir and Price 2011; Tobias et al. 2014). To control for variation in the evolutionary distance
787 between sister taxa, "sister taxa GLMs" include patristic distance as a predictor in non-
788 phylogenetic regressions (e.g., Davies *et al.* 2007; Martin *et al.* 2010).
789
790 *8. Sister-taxa model fitting*
791 Recently, tools have been described for fitting process-based models to sister taxa
792 datasets using maximum likelihood (Weir and Wheatcroft 2011; Weir and Lawson 2015). With
793 these tools, it is possible to test whether models that allow evolutionary rates to vary as a linear
794 function of a gradient (e.g., whether male plumage coloration varies as a function of the strength
795 of sexual selection, Seddon et al. 2013) better fit sister-taxa datasets than constant rates models.
796 When the gradient is the number of sympatric lineages, these models are conceptually similar to
797 the linear diversity dependent models described above.

Supporting Information for "An assessment of phylogenetic tools for analyzing the interplay between interspecific interactions and phenotypic evolution"

Drury, J.P., Grether, G.F., Garland, Jr., T., & Morlon, H.

1. Supplementary Methods

2. Supplementary Tables 1 & 2

3. Supplementary Figures 1-17

SUPPLEMENTARY METHODS

Simulating Phylogenies Under Varying Biogeographic Scenarios

Joint simulation of trees and biogeographies requires parameterizing (1) the diversification process (the rules defining how new species appear), (2) rates of anagenetic range gains/losses (the rules defining how lineages' ranges change), and (3) cladogenetic range inheritance (the rules defining how two sister lineages divide their ancestral range upon speciation). In each scenario, we evolved species ranges under the DEC+J model (Matzke 2014) across a grid of ten possible regions with equal probability of transitions between regions and only one region occupied at the root of the tree. We simulated the diversification process along each tree with a rate of 0.25 (speciation/lineage/time unit). Anagenetic changes were simulated under two dispersal rates {d (transition/lineage/unit time) = 0.03, 0.06}, chosen from within a range of dispersal values estimated from empirical datasets. When anagenetic dispersal happens, a lineage occupies an additional region chosen at random. Across these two values of "d", we held local extirpation rates constant at e = 0.03 (local extirpation/lineage/unit time), the median value used for simulations in Matzke 2014. In cases where a lineage occupying only one region goes locally extinct, that lineage goes extinct (Matzke 2014).

The cladogenetic events possible in the DEC+J model are—briefly (for a detailed explanation of each of these processes, see Matzke 2014)— sympatric speciation (both daughter lineages keep the one-region ancestral range, parameter "y"), subset sympatric speciation (one of the daughter lineages keeps the ancestral range, the other one inherits a subset of the ancestral range, parameter "s"), vicariance (the two daughter lineages split the ancestral range, parameter "v"), and founder event speciation (one daughter lineages keeps the ancestral range, the other occupies a new region, parameter "j").

As the pool of possible daughter ranges changes depending on the ancestral range (e.g., there are fewer ways in which the ancestral two-region range "AB" can be propagated to daughter lineages than the three-range region "ABC"), cladogenetic range changes are sampled by first assigning each type of cladogenetic change (y,s,v, and j from above) a particular weight. From these weighted ranges, the probability that a daughter inherits a specific range is calculated by dividing the weight assigned to that range by the sum of the weights of each possible daughter range (Matzke 2014). By default, the relative weight of sympatric speciation (range copying), subset sympatric speciation, and vicariance are equal in most implementations of the DEC model (i.e., y=s=v). To generate biogeographic scenarios where recently diverged sister taxa are more likely to be allopatric, we implemented a scenario where the weight of either type of sympatric speciation event is very low {y = s = 0.005*v} as well as under default parameter values {y = s = v}. Across both scenarios, we held the relative weight of founder event speciation constant (j = 0.1, y + s + v = 2.9).

Simulating Character Displacement

Datasets were simulated under Eq. 1 in the main text as follows:
1. At the first time step (the root), the trait value was set to z_0 (= 0 in all cases).
2. Each time step *dt* was set to the total tree height divided by 2500. To complete the simulation along any branch not divisible by this value of *dt*, we set the time step equal to the remainder of the branch length divided by *dt*.

3. During each time step from the root to the tip of the tree, the trait value of lineage *i* is calculated according to Eq 1. For the component of Eq.1 dictating the magnitude of divergence or convergence, between-lineage distances in trait space were calculated based on similarity at time *t-dt*. In simulations of divergent character displacement, if species have identical trait values, the "sign" value is overridden so that species move in the opposite direction of one another in trait space.
4. At a branching event, the trait values of both daughter lineages are set to equal the value of the parent lineage.

For divergent character displacement scenarios, we arbitrarily chose simulation parameter values based on visual inspection of simulated trajectories under different combinations of parameter values. We chose to focus on $m = 2$, and also explored the effect of varying this parameter between 1 & 10, because we could visualize divergence in the realized simulations. For example, for a 20 tip tree simulated with high dispersal and low sympatric speciation:

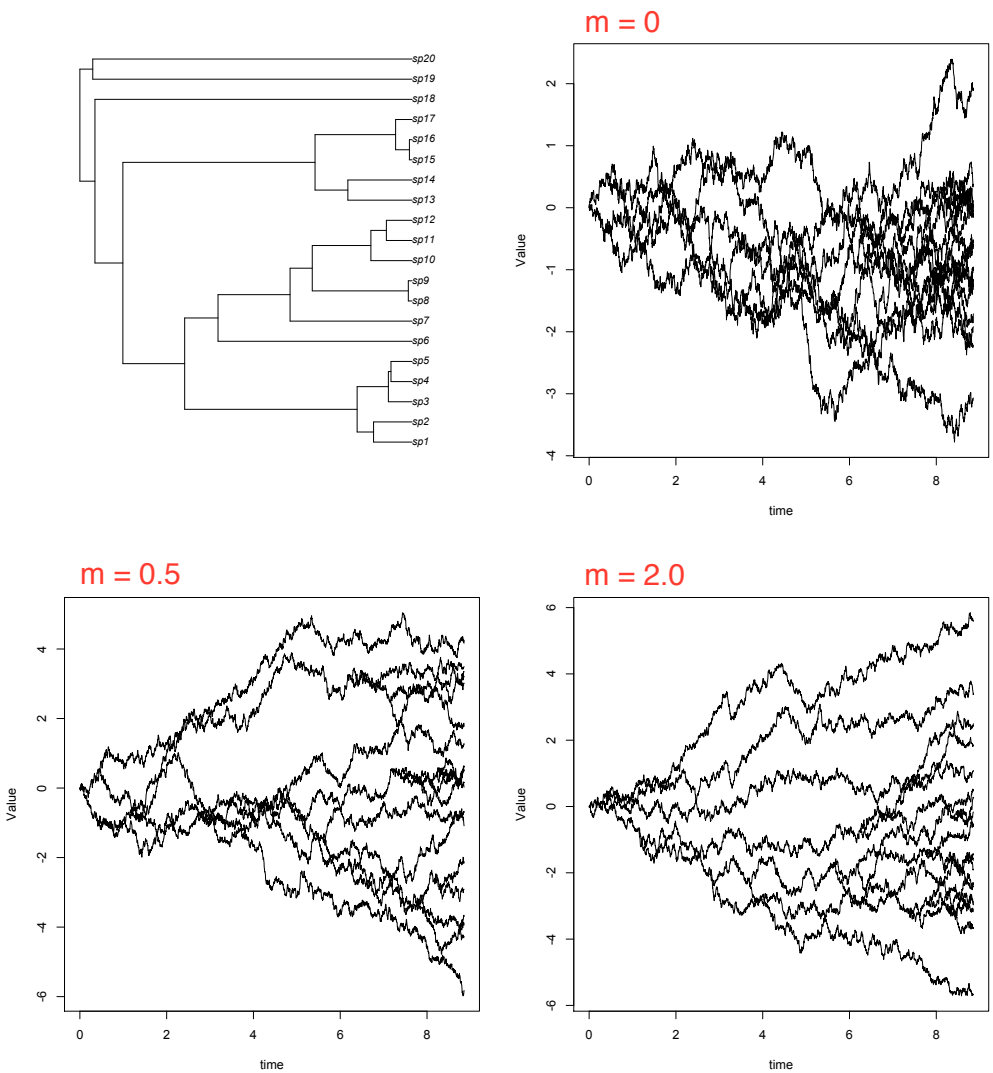

In convergent character displacement simulations, we likewise chose parameter values based on visual inspection of simulated trajectories under different combinations of parameter values. We chose to focus on *m* = -0.25, and also explored the effect of varying this parameter between -0.1 & -0.50, because we could visualize convergence in the realized simulations and the simulated trait values did not converge across the entire clade. For example, on the same tree as above:

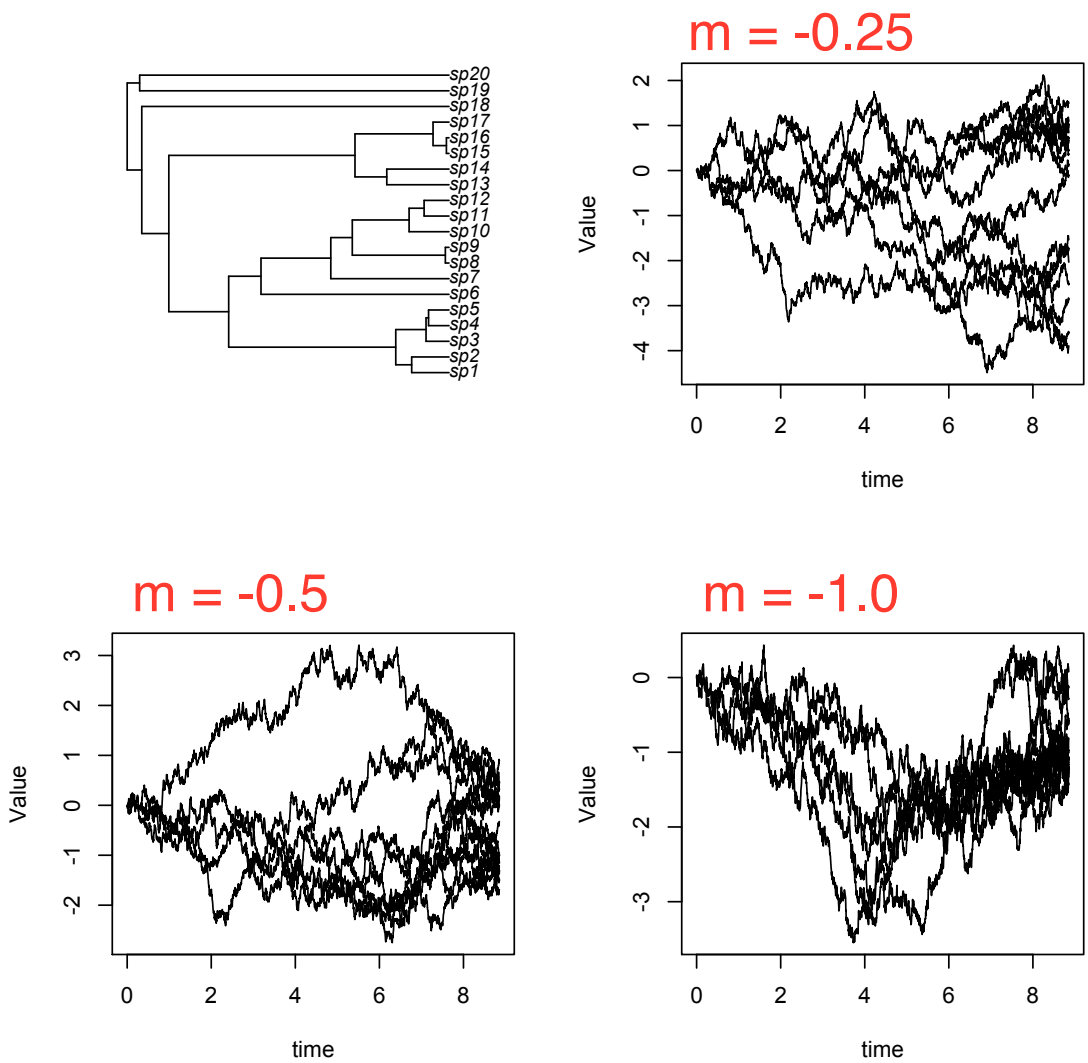

Analytical Methods

Non-phylogenetic regressions: General Linear Models (GLMs) were fitted to simulated datasets using the glm function in R. For character displacement analyses, linear models were fit to pairwise differences in trait data, with sympatry/allopatry as the predictor variable. For interaction analyses, logistic regressions were fit to the simulated species interaction variable, with pairwise difference in the focal trait as the predictor variable.

Mantel tests: We computed raw Mantel tests using mantel.rtest in ade4 (Dray and Dufour 2007), specifying 1000 permutations to assess statistical significance. We computed phylogenetically permuted partial Mantel (pppMantel) tests (Lapointe and Garland 2001) using the script phyloMantel.R from Harmon & Glor (2010), again using 1000 permutations to test for significance.

Phylogenetic linear mixed models (PLMMs): For the character displacement datasets, we fitted PLMMs using asreml-R (Butler et al. 2009), including both sympatry and the patristic distance (calculated using the cophenetic.phylo function in ape [Paradis 2011]) between each pairwise species comparison as fixed effects and including the identity of each lineage and the phylogeny as random effects, following Tobias *et al.* (2014). To assess statistical significance of the fixed effects, we used Wald-type F-tests with Kenward-Rogers adjustments to the denominator degrees of freedom using the wald.asreml function with the option denDF = "numeric" in asreml-R, again following Tobias *et al*. (2014)

For the scenario using traits to predict species interactions, we fit PLMMs using MCMCglmm in R (Hadfield 2010), because the residual maximum likelihood approach used in asreml-R may bias estimates for logistic regressions (Bolker et al. 2009). We used standard inverse-Gamma priors for the fixed and random effects, using the code:

```
prior<-list(G=list(G1=list(V=1,nu=0.002),G2=list(V=1,nu=0.002),G3=list(V=1,nu=0.002)),R=list(V=1,nu=0.02))
```

We ran each fit for between 2 million and 20 million chains based on preliminary assessment of convergence for different tree sizes, varying the burn-in and thinning periods to result in approximately 2000 runs. We visually inspected convergence for a large sample of model fits to make sure that our MCMC parameterization was working well. MCMC fits were very computationally expensive, so we fit the models to a subset of simulated datasets (n = 100 per tree size, biogeography, and simulation parameter combination).

For all PLMMs, we randomized the order in which the identity of the lineages was passed to the random effects.

Simulation approach: BM models were first fit to simulated trait data using mvBM in the mvMORPH package (Clavel et al. 2015). Then, 5,000 datasets were simulated using the maximum likelihood estimate of the BM rate parameter and state at the root using fastBM in phytools (Revell 2012). A GLM (as outlined in "non-phylogenetic regressions", the predictor variable for character displacement analyses was biogeographical overlap and the response variable was pairwise trait similarity, and for analyses of species interactions, the pairwise trait similarity was the predictor variable and a binomial variable of species interaction was the response variable) was fit to each of these simulated datasets, and the resulting analysis was considered statistically significant if both (a) the non-phylogenetic test on the raw data was statistically significant and (b) the test statistic from the raw analysis was outside of the 2.5-97.5% quantile interval of test statistics estimated on the simulated datasets.

Sister taxa analyses: for trees of size 150 and larger, we culled sister taxa from the full trees. We then ran non-phylogenetic regressions, PLMMs, the simulation approach and sister taxa GLMs on the culled dataset.

Phenotypic models: We fit all phenotypic models by maximum likelihood. We fit BM and OU models using geiger (Pennell et al. 2014) and the matching competition and two diversity dependent models (with either linear or exponential dependence of sigma on the number of species) using RPANDA (Morlon et al. 2016) in R. For the latter models, we included the biogeography used to simulate the datasets in the model fits, as described in Drury *et al.* (2016). We then compared the relative support of these models using Akaike weights (Burnham and Anderson 2002), since the models are not nested. Since model-fitting is computationally expensive, we fit the process-based models to a subset of datasets simulated on 100 tip trees (n = 100 biogeography and simulation parameter combination).

Additionally, to analyze the effect of m and ψ on rates of evolution, we fit four trait models to the sister-taxa datasets for both divergent and convergent character displacement scenarios using the R package EvoRAG (Weir and Lawson 2015): BM, OU, plus versions of BM and OU that allow the rate of trait evolution to change with the number of sympatric lineages (i.e., "BM_null", "OU_null", "BM_linear", and "OU_linear_beta").

SUPPLEMENTARY REFERENCES

Bolker, B. M., M. E. Brooks, C. J. Clark, S. W. Geange, J. R. Poulsen, M. H. H. Stevens, and J.-S. S. White. 2009. Generalized linear mixed models: a practical guide for ecology and evolution. Trends Ecol. Evol. 24:127–135. Elsevier.

Burnham, K. P., and D. R. Anderson. 2002. Model selection and multimodel inference: a practical information-theoretic approach. 2nd editio. Springer, New York, NY.

Butler, D., B. Cullis, A. Gilmour, and B. Gogel. 2009. ASReml user guide release 3.0. VSN Int. Ltd, Hemel Hempstead, UK.

Clavel, J., G. Escarguel, and G. Merceron. 2015. mvMORPH: an R package for fitting multivariate evolutionary models to morphometric data. Methods Ecol. Evol. 6:1311–1319. Wiley Online Library.

Dray, S., and A. B. Dufour. 2007. The ade4 package: implementing the duality diagram for ecologists. J. Stat. Softw. 22:1–20.

Drury, J., J. Clavel, M. Manceau, and H. Morlon. 2016. Estimating the effect of competition on trait evolution using maximum likelihood inference. Syst. Biol. 65:700–710.

Hadfield, J. D. 2010. MCMC methods for multi-response generalized linear mixed models: the MCMCglmm R package. J. Stat. Softw. 33:1–22.

Harmon, L. J., and R. E. Glor. 2010. Poor statistical performance of the Mantel test in phylogenetic comparative analyses. Evolution (N. Y). 64:2173–2178.

Lapointe, F. J., and T. Garland. 2001. A generalized permutation model for the analysis of cross-species data. J. Classif. 18:109–127. Springer.

Matzke, N. J. 2014. Model selection in historical biogeography reveals that founder-event speciation is a crucial process in island clades. Syst. Biol. 63:951–970.

Morlon, H., E. Lewitus, F. L. Condamine, M. Manceau, J. Clavel, and J. Drury. 2016. RPANDA: an R package for macroevolutionary analyses on phylogenetic trees. Methods Ecol. Evol. 7:589–597. Wiley Online Library.

Paradis, E. 2011. Analysis of Phylogenetics and Evolution with R. Springer, New York, NY.

Pennell, M. W., J. M. Eastman, G. J. Slater, J. W. Brown, J. C. Uyeda, R. G. FitzJohn, M. E. Alfaro, and L. J. Harmon. 2014. geiger v2. 0: an expanded suite of methods for fitting macroevolutionary models to phylogenetic trees. Bioinformatics btu181. Oxford Univ Press.

Revell, L. J. 2012. phytools: An R package for phylogenetic comparative biology (and other things). Methods Ecol. Evol. 3:217–223.

Tobias, J. A., C. K. Cornwallis, E. P. Derryberry, S. Claramunt, R. T. Brumfield, and N. Seddon. 2014. Species coexistence and the dynamics of phenotypic evolution in adaptive radiation. Nature 506:359–363. Nature Publishing Group.

Weir, J. T., and A. Lawson. 2015. Evolutionary rates across gradients. Methods Ecol. Evol. 6:1278–1286.

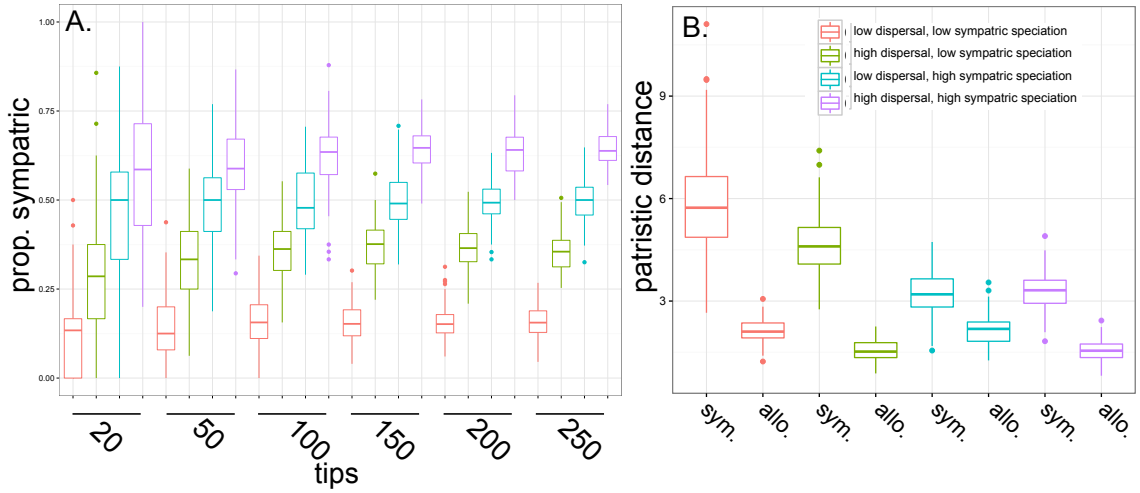

Supplementary Figure 1. The resulting biogeographic landscape under each of the four biogeographic scenarios. A. The proportion of sister taxa that are living in sympatry varies as a function of both the dispersal rate and the level of sympatric speciation. B. The patristic distances (the branch lengths separating sister taxa) are larger for sympatric taxa, although the magnitude of this difference depends on the biogeographic scenario.

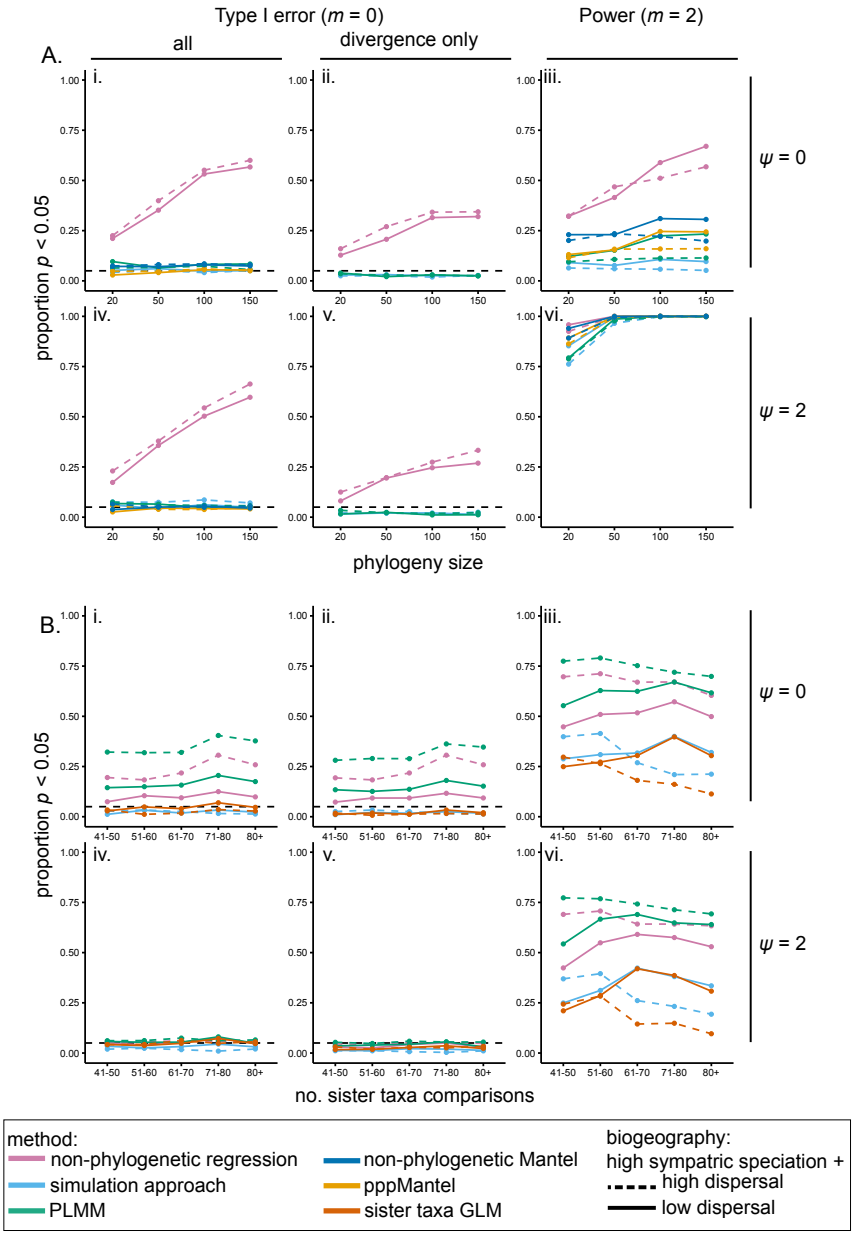

Supplementary Figure 2. Proportion of statistically significant analyses in datasets simulated under divergent character displacement in biogeographic scenarios with high sympatric speciation rates. A. Results from approaches using data from all pairwise comparisons in a clade, plotted as a function of the phylogeny size and dispersal rate when i-ii. $m = 0$ and $\psi = 0$ (i. all analyses and ii. only analyses returning divergence in sympatry), iii. $m = 2$ and $\psi = 0$, iv-v. $m = 0$ and $\psi = 2$ (iv. all analyses and v. only analyses returning divergence in sympatry), and vi. $m = 2$ and $\psi = 2$. B. Results from analyses of sister-taxa culled from complete phylogenies binned by the number of resulting species pairs, plotted as a function of the number of sister taxa comparisons and dispersal rate when i-ii. $m = 0$ and $\psi = 0$ (i. all analyses and ii. only analyses returning divergence in sympatry), iii. $m = 2$ and $\psi = 0$, iv-v. $m = 0$ and $\psi = 2$ (iv. all analyses and v. only analyses returning divergence in sympatry), and vi. $m = 2$ and $\psi = 2$. For scenarios where $m = 2$, only the proportion of significant results showing divergence are plotted. Dashed horizontal lines represent a Type I error rate of 5%.

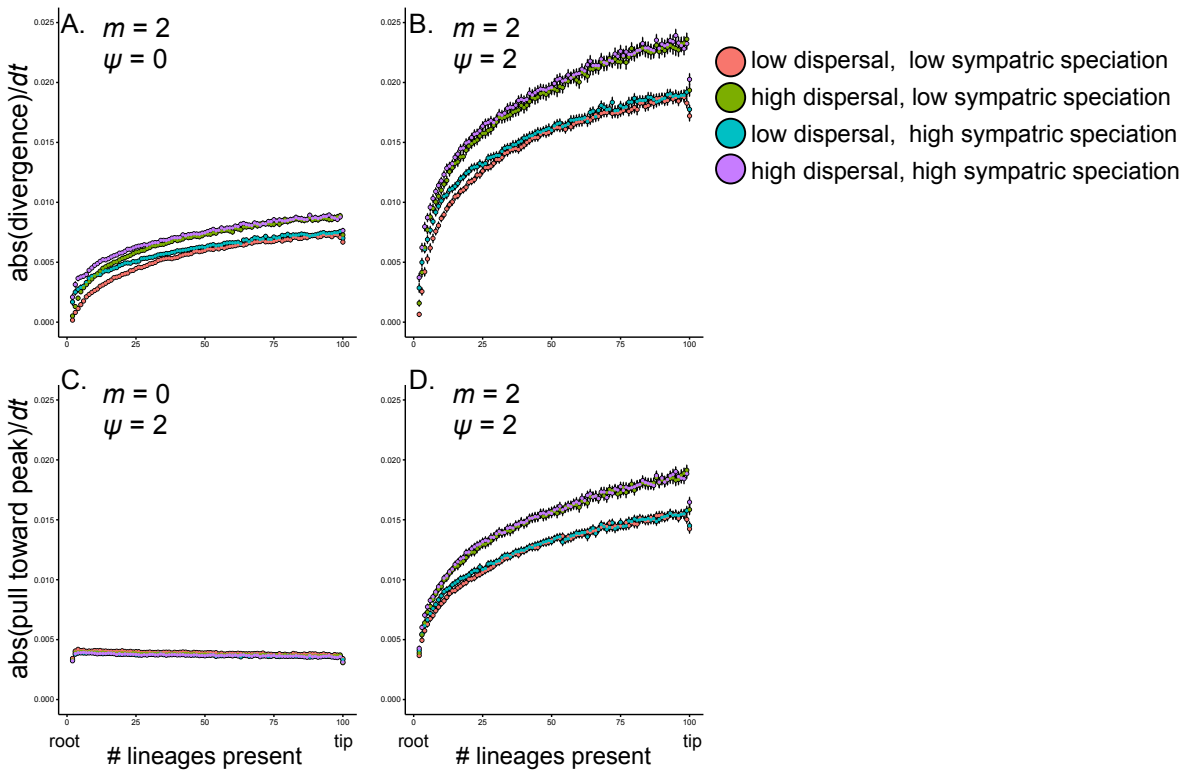

Supplementary Figure 3. The effect of repulsion on the magnitude of changes in traits from the root to the tip of phylogenies under different simulation scenarios. To calculate the absolute value of divergence steps (A & B), we recorded the absolute value of the magnitude of the step size resulting from the deterministic repulsion step of Eq. 1 (i.e., $m\left[\sum_{j\neq i}^{n}\mathbf{A}_{i,j}\times sign\left(z_i(t)-z_j(t)\right)\times e^{-\alpha\left(y_j(t)-y_i(t)\right)^2}\right]dt$) at each time step, took the mean during each internode interval for all extant lineages within trees, and then averaged each internode interval across all simulations. Each point thus represents the mean of means and the standard error across 100 phylogenies. The absolute value of the steps pulling trait values toward a stable peak (C & D) similarly represents the absolute value of the magnitude of the step size resulting from the deterministic component of the OU attraction to the peak in Eq. 1 (i.e., $\psi\left(\theta-z_i(t)\right)dt$).

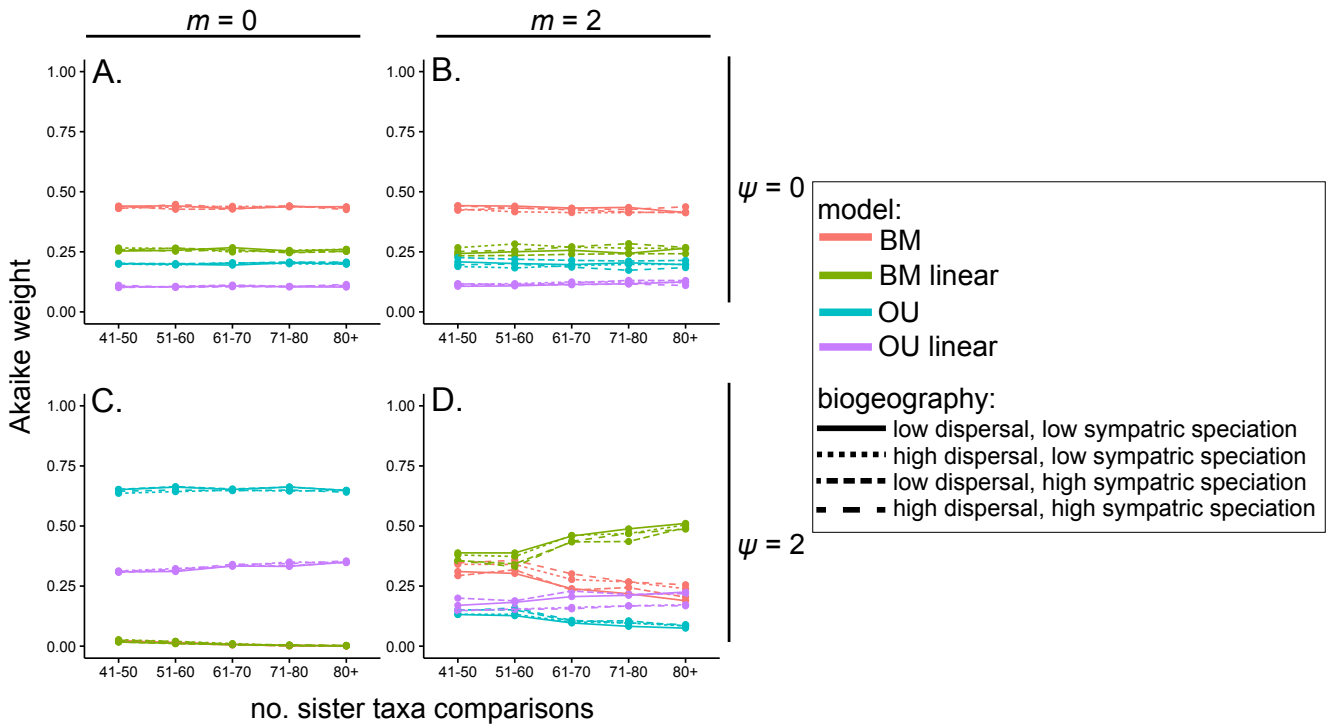

Supplementary Figure 4. Models fit to sister-taxa datasets generated under divergent character displacement scenarios in EvoRAG corroborate the influence of the number of sympatric lineages on the rate of evolution. A. When $\psi = 0$, BM is the best fitting model, whether A. $m = 0$ or B. $m = 2$. When $\psi = 2$, OU is the best fitting model when C. $m = 0$, whereas a BM model that allows the rate of trait evolution to vary linearly with the number of sympatric lineages is a best fitting model when D. $m = 2$. Plots depict the Akaike weight of each model as a function of both the biogeographic scenario and the number of sister taxa comparisons.

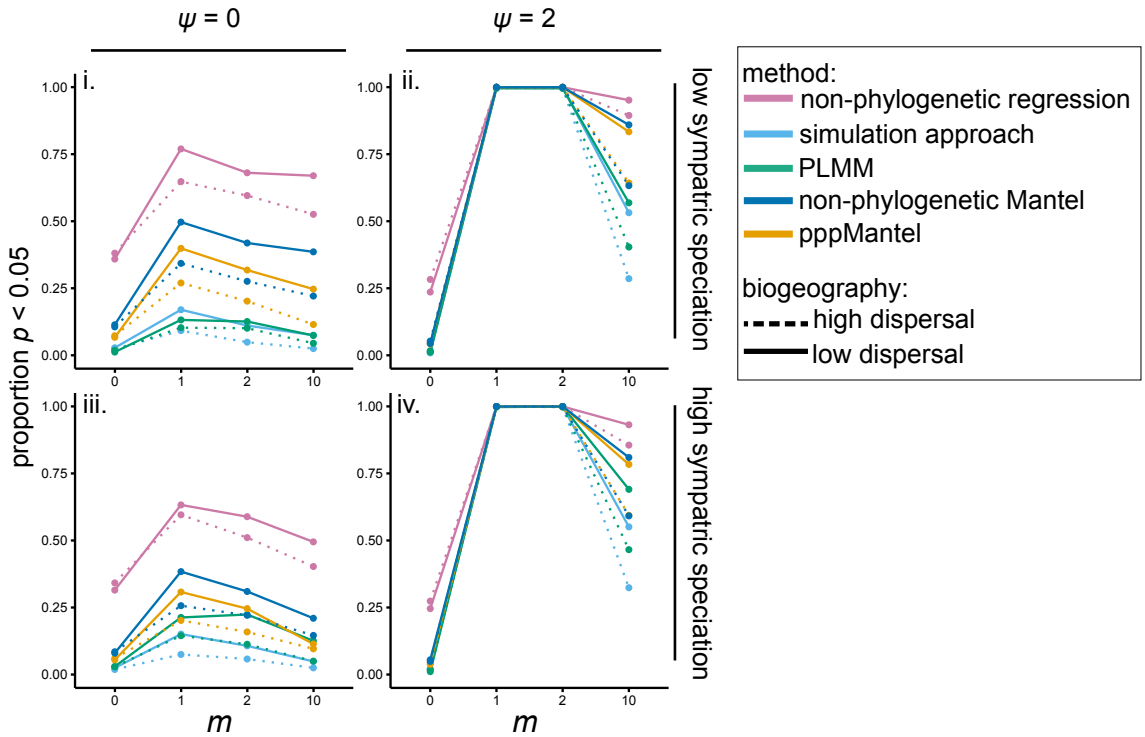

Supplementary Figure 5. The proportion of statistically significant analyses for datasets with divergent character displacement varies as a function of both *m* and *ψ*.

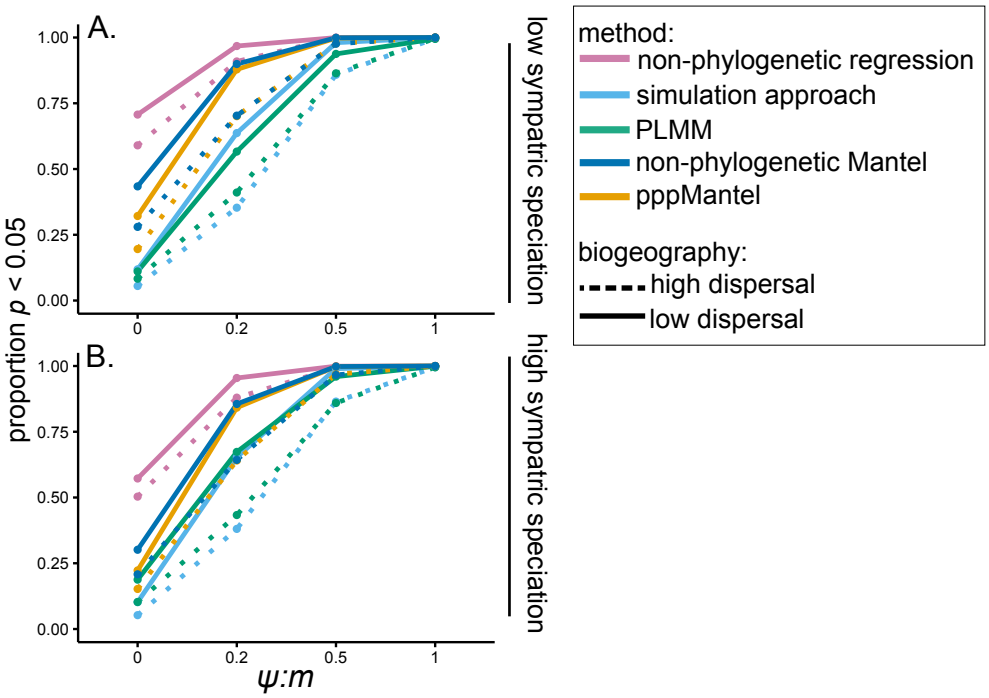

Supplementary Figure 6. As *ψ:m* increases, the ability of all methods to detect character displacement, when present, increases under both low sympatric speciation (A) and high sympatric speciation (B) scenarios.

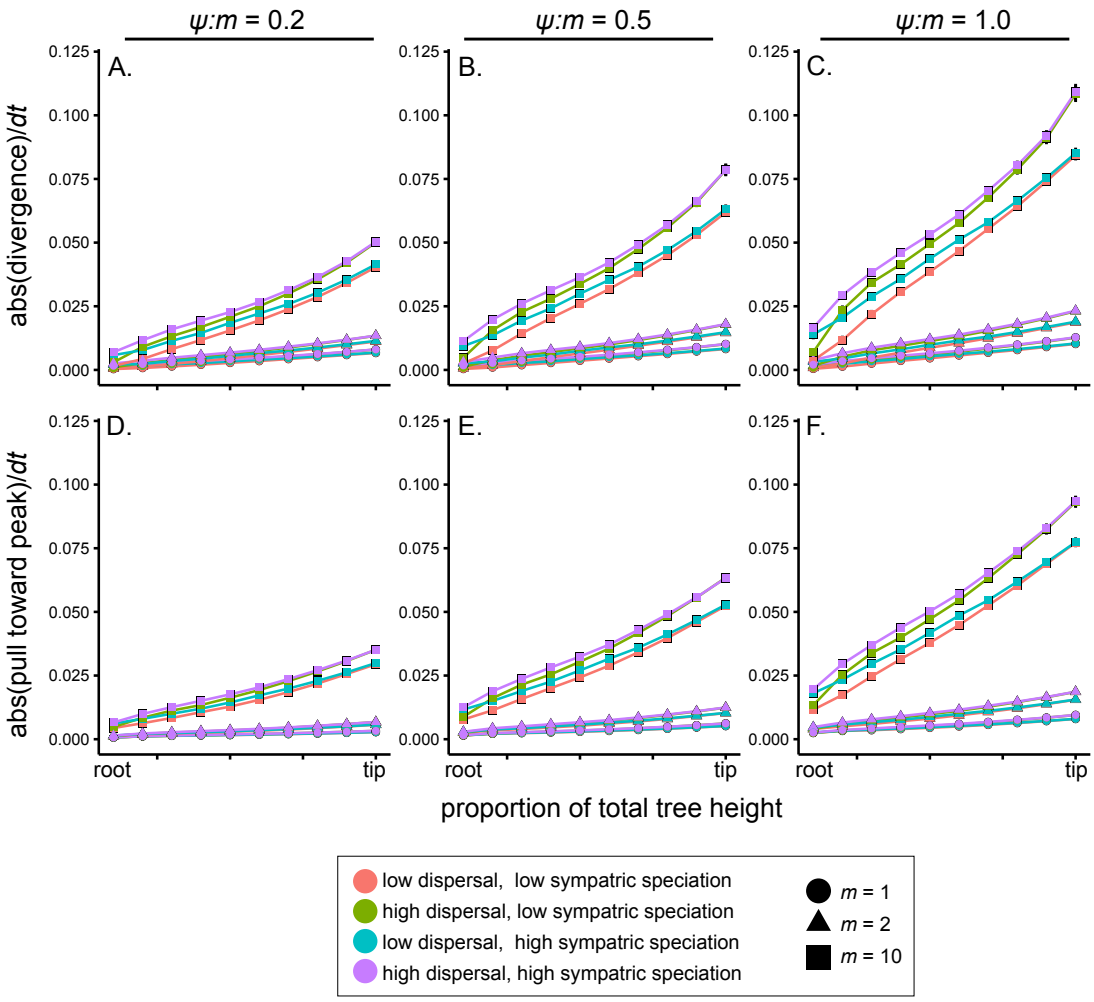

Supplementary Figure 7. The effect of repulsion on the magnitude of changes in traits from the root to the tip of phylogenies as a function of the ratio ψ:m. As ψ increases relative to m, both the magnitude of divergence steps (panels A-C) and the magnitude of the steps pulling trait values toward the peak (panels D-F) increase. This effect becomes increasingly apparent at higher m values and in biogeographic scenarios generated under high dispersal rates. For a description of the data, see the legend of Fig. S3. In this plot, data are averaged within 10 time bins representing each 10% of the total height of the phylogeny.

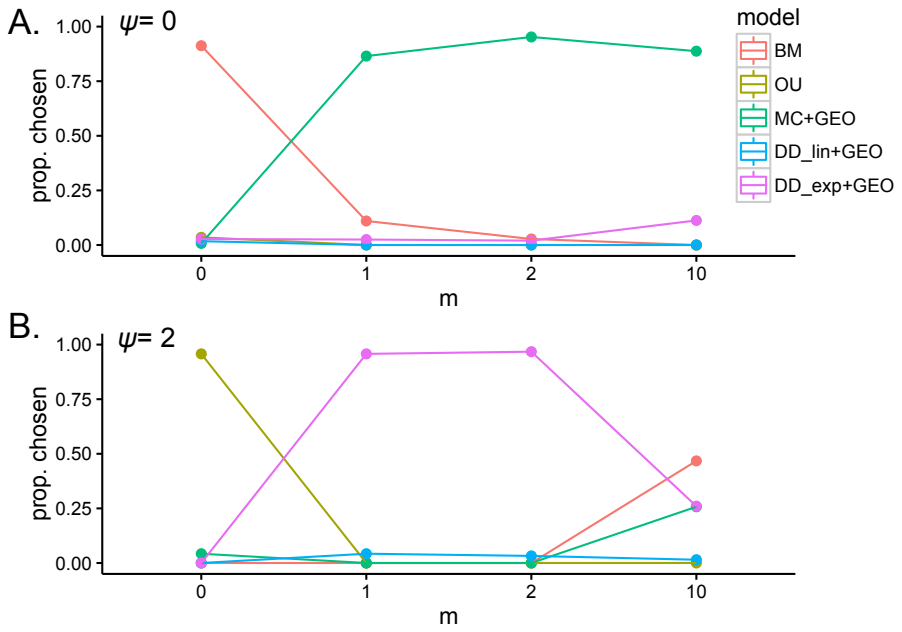

Supplementary Figure 8. Proportion of simulated datasets for which a given phenotypic model was chosen using model selection as a function of *m*. We considered a model to be chosen if it had the lowest AICc score among all of the models, and if the AICc score was > 2 units away from BM model. A. Results for datasets simulated without the OU process. B. Results from datasets simulated with $\psi = 2$.

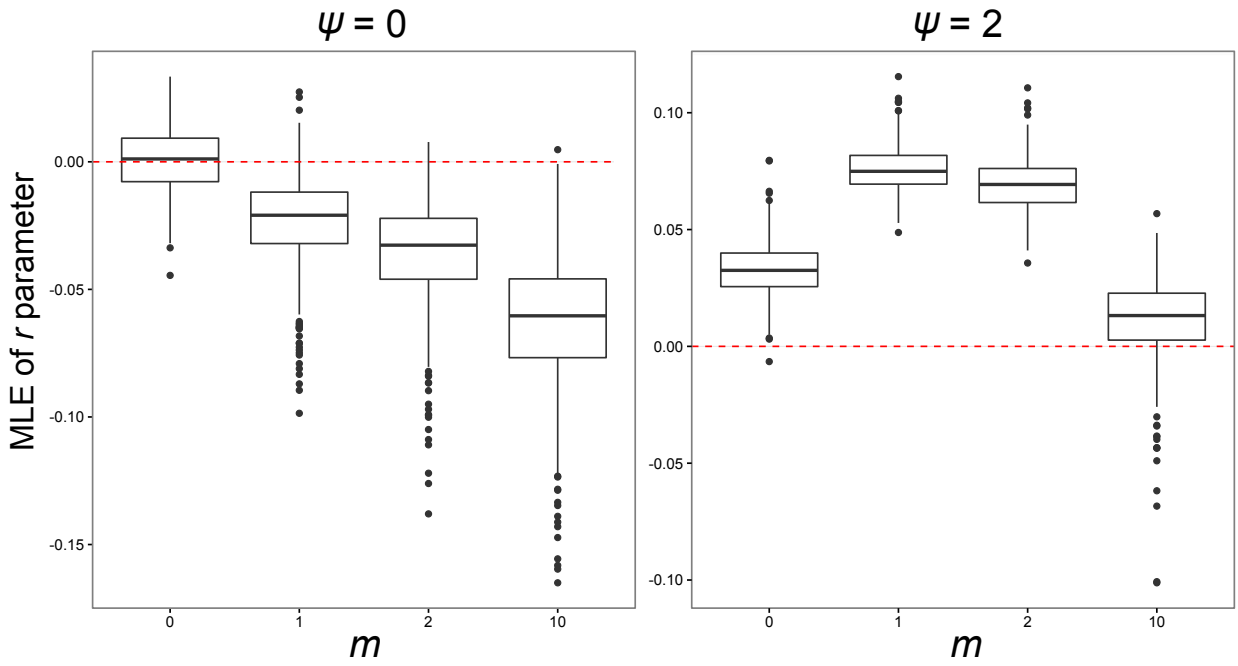

Supplementary Figure 9. The rate parameter r of the DDexp+GEO model is increasingly negative with increasing m values when $\psi = 0$, yet is positive when $\psi > 0$.

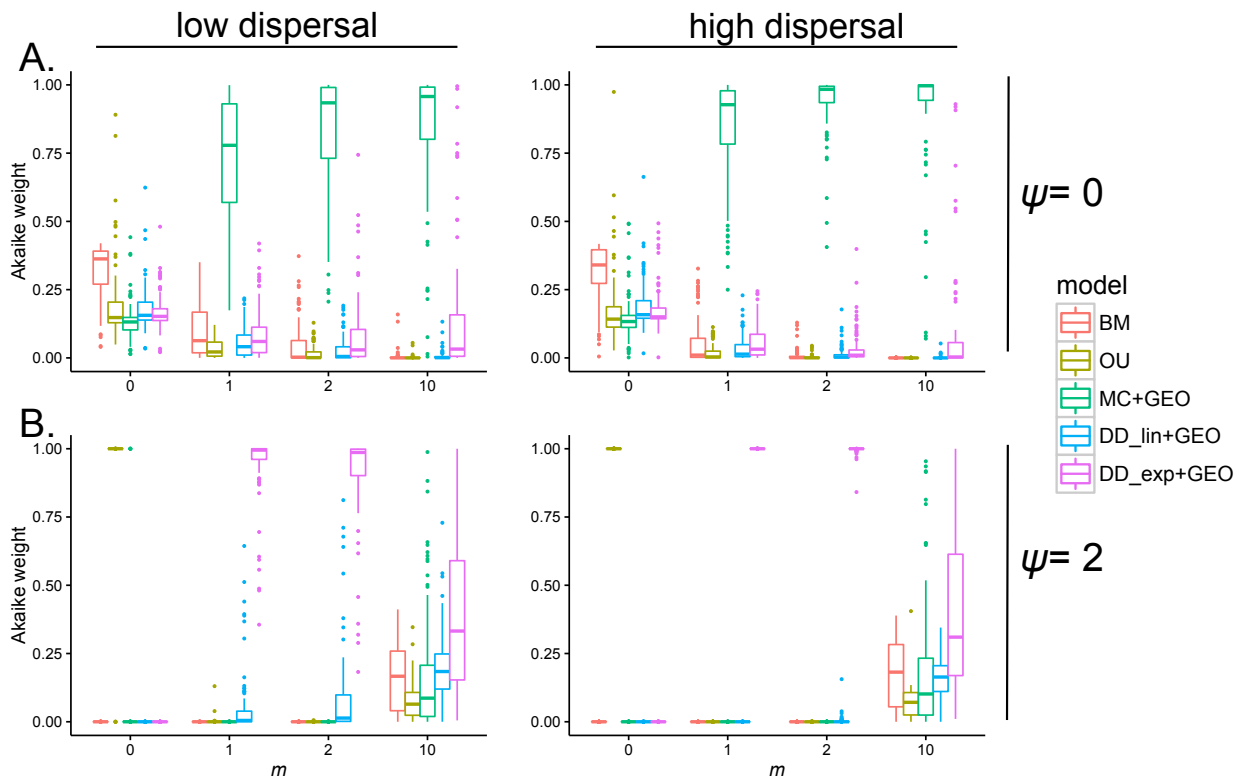

Supplementary Figure 10. Akaike weights for each trait model fit to simulated datasets in biogeographic scenarios with high sympatric speciation rates as a function of *m*. A. When OU is absent, BM is the best-fit model when $m = 0$, and the matching competition model with biogeography is the best model when competitive divergence is present. B. When OU is present, OU is the best-fit model when $m = 0$, and the diversity-dependent exponential model with biogeography is the best model when competitive divergence is present and ψ:m is relatively high.

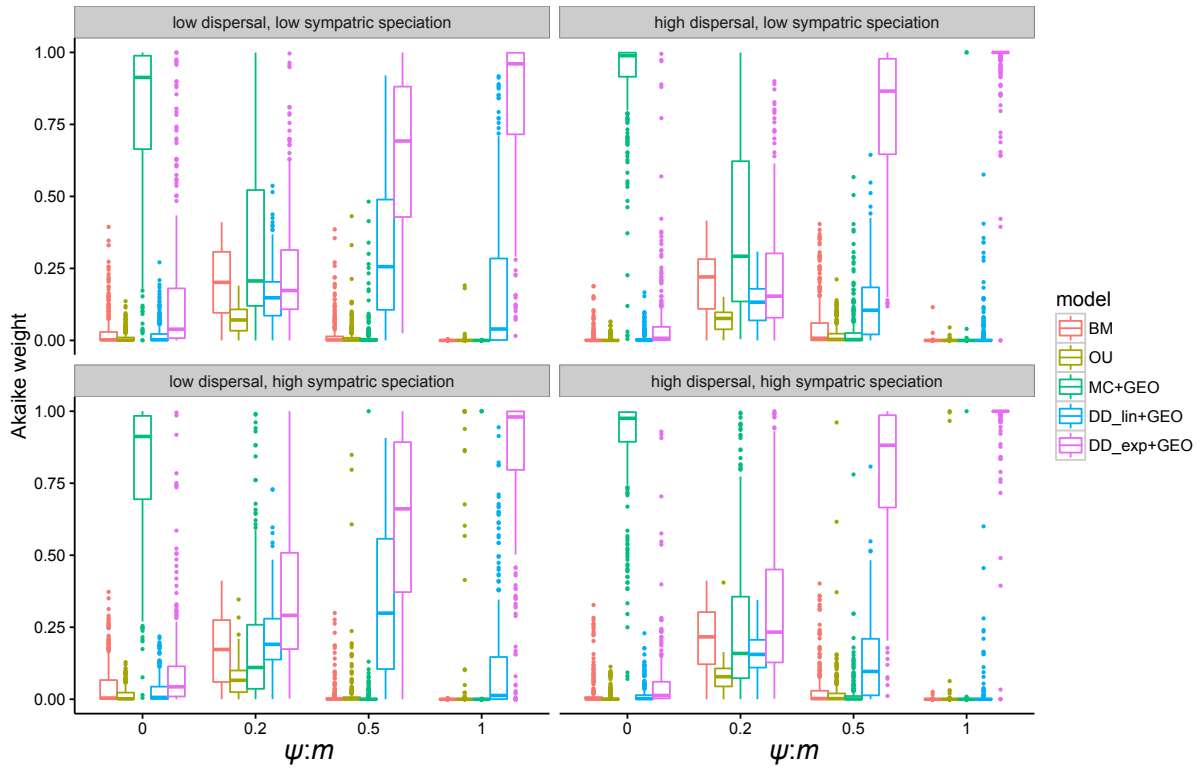

Supplementary Figure 11. As ψ:m increases, the DDexp + GEO model is increasingly better fit to datasets simulated with character displacement.

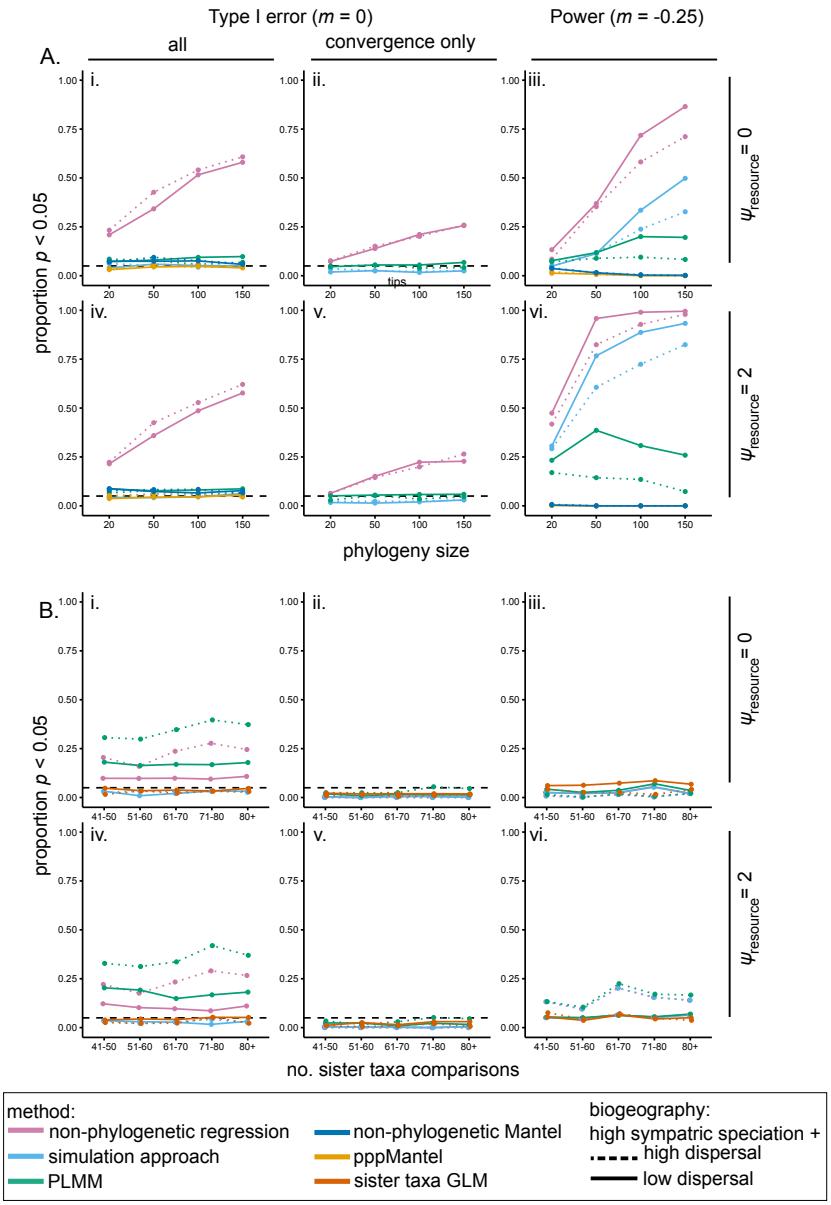

Supplementary Figure 12. Proportion of statistically significant analyses in datasets simulated under convergent character displacement in biogeographic scenarios with high sympatric speciation rates. A. Results from approaches using data from all pairwise comparisons in a clade, plotted as a function of the phylogeny size and dispersal rate when i-ii. $m = 0$ and $\psi_{resource} = 0$ (i. all analyses and ii. only analyses returning convergence in sympatry), iii. $m = -0.25$ and $\psi_{resource} = 0$, iv-v. $m = 0$ and $\psi_{resource} = 2$ (iv. all analyses and v. only analyses returning convergence in sympatry), and vi. $m = -0.25$ and $\psi_{resource} = 2$. B. Results from analyses of sister-taxa culled from complete phylogenies binned by the number of resulting species pairs, plotted as a function of the number of sister taxa comparisons and dispersal rate when i-ii. $m = 0$ and $\psi_{resource} = 0$ (i. all analyses and ii. only analyses returning convergence in sympatry), iii. $m = -0.25$ and $\psi_{resource} = 0$, iv-v. $m = 0$ and $\psi_{resource} = 2$ (iv. all analyses and v. only analyses returning convergence in sympatry), and vi. $m = -0.25$ and $\psi_{resource} = 2$. For scenarios where $m = -0.25$, only the proportion of significant results showing convergence are plotted. Dashed horizontal lines represent a Type I error rate of 5%.

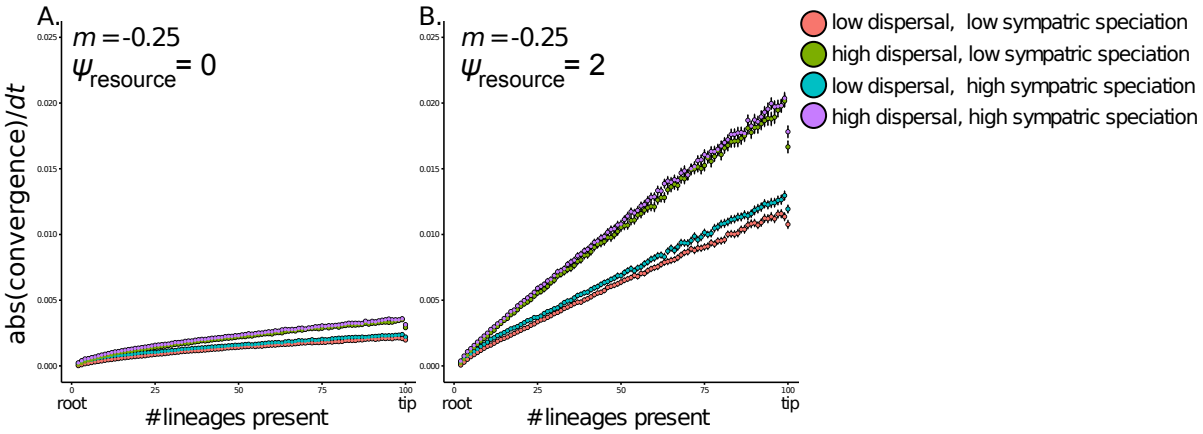

Supplementary Figure 13. The effect of convergence on the magnitude of changes in traits in simulations, plotted as a function of stabilizing selection in the resource-use trait ($\psi_{resource}$) and biogeography. With $\psi_{resource} = 2$, the magnitude of convergence steps is higher, and this is particularly true for high dispersal biogeographies. Data generated as described in the legend of Fig. S3.

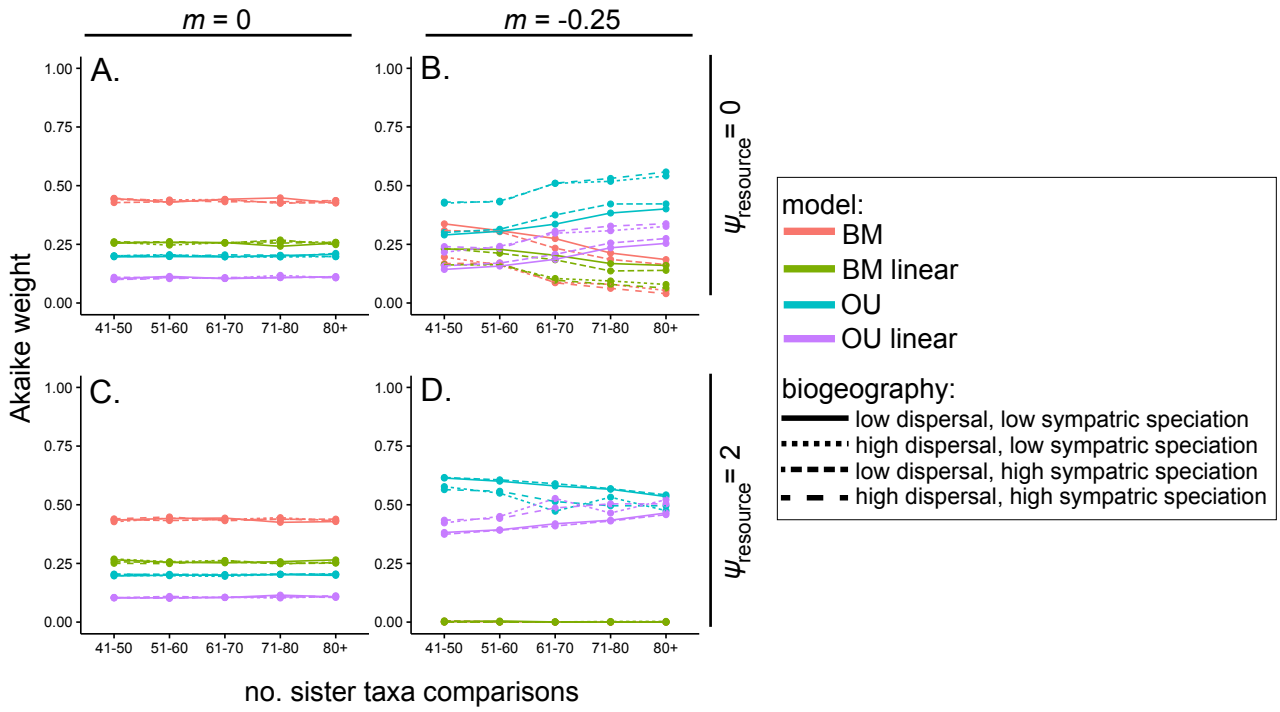

Supplementary Figure 14. Models fit to sister-taxa datasets generated under convergent character displacement scenarios in EvoRAG. A. When $m = 0$, BM is the best fitting model, whether A. $\psi_{resource} = 0$ or C. $\psi_{resource} = 2$. When $m = -0.25$, OU is the best fitting model when C. $\psi_{resource} = 0$ and D. $\psi_{resource} = 2$, but an OU model with evolutionary rates that change linearly as a function of the number of sympatric lineages (OU linear) is also a strong model. Plots depict the Akaike weight of each model as a function of both the biogeographic scenario and the number of sister taxa comparisons.

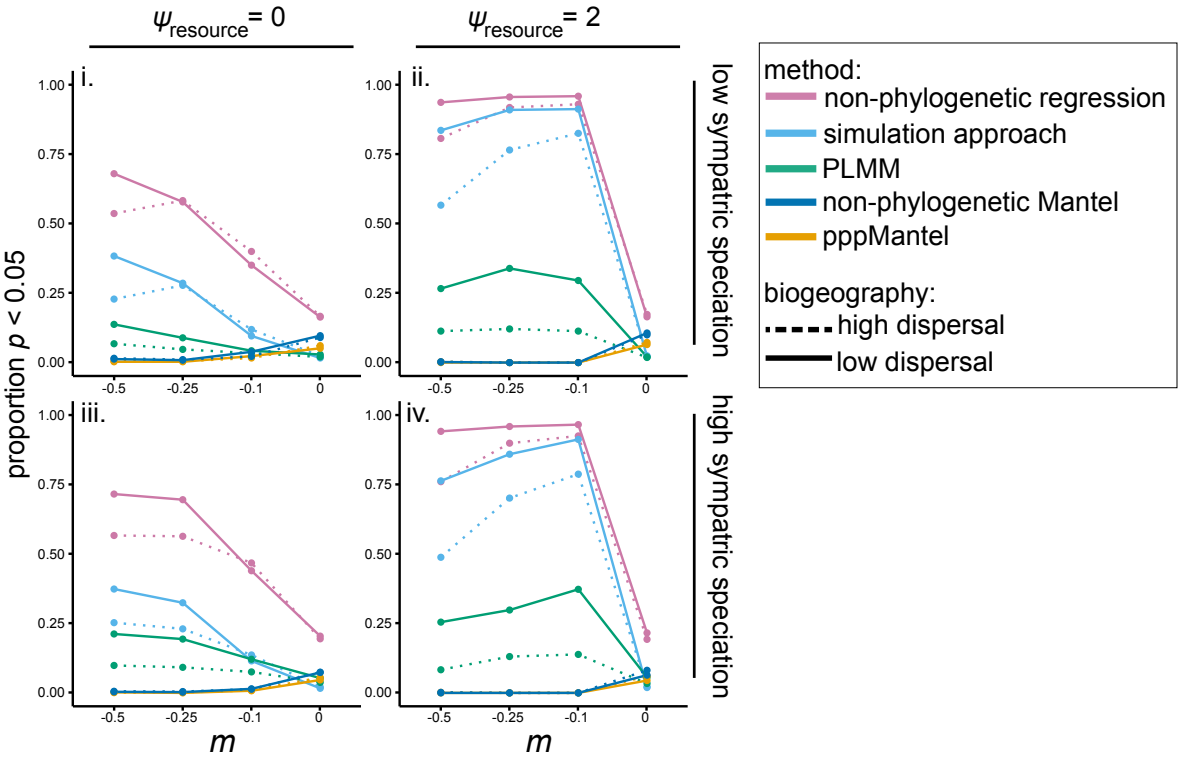

Supplementary Figure 15. The proportion of statistically significant analyses for datasets with convergent character displacement varies as a function of both *m*, and is generally lower in the absence of a pull toward a peak (i,iii) compared to cases where data were simulated with a pull toward a peak (ii,iv).

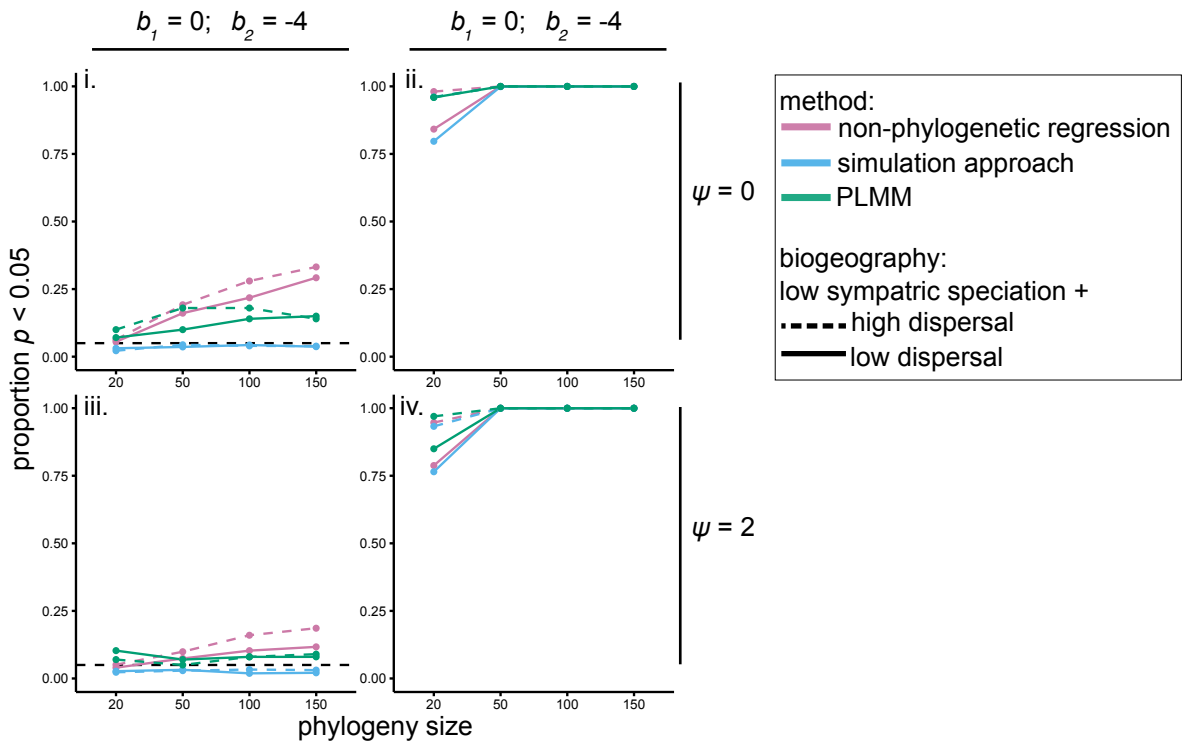

Supplementary Figure 16. Proportion of statistically significant analyses in datasets with interactions simulated under a simple phenotype matching process in biogeographic scenarios with high sympatric speciation rates. Results from analyses where the focal trait was simulated under A. BM or B. OU, plotted as a function of the dispersal rate when i. b_1 (the simulation coefficient determining the relationship between the interaction and the measured trait) = 0, b_2 (the simulation coefficient for an unmeasured trait) = -4, and ψ = 2, ii. b_1 = -4, b_2 = 0, and ψ = 2, iii. b_1 = 0, b_2 = -4, and ψ = 0, and iv. b_1 = -4, b_2 = 0, and ψ = 0.

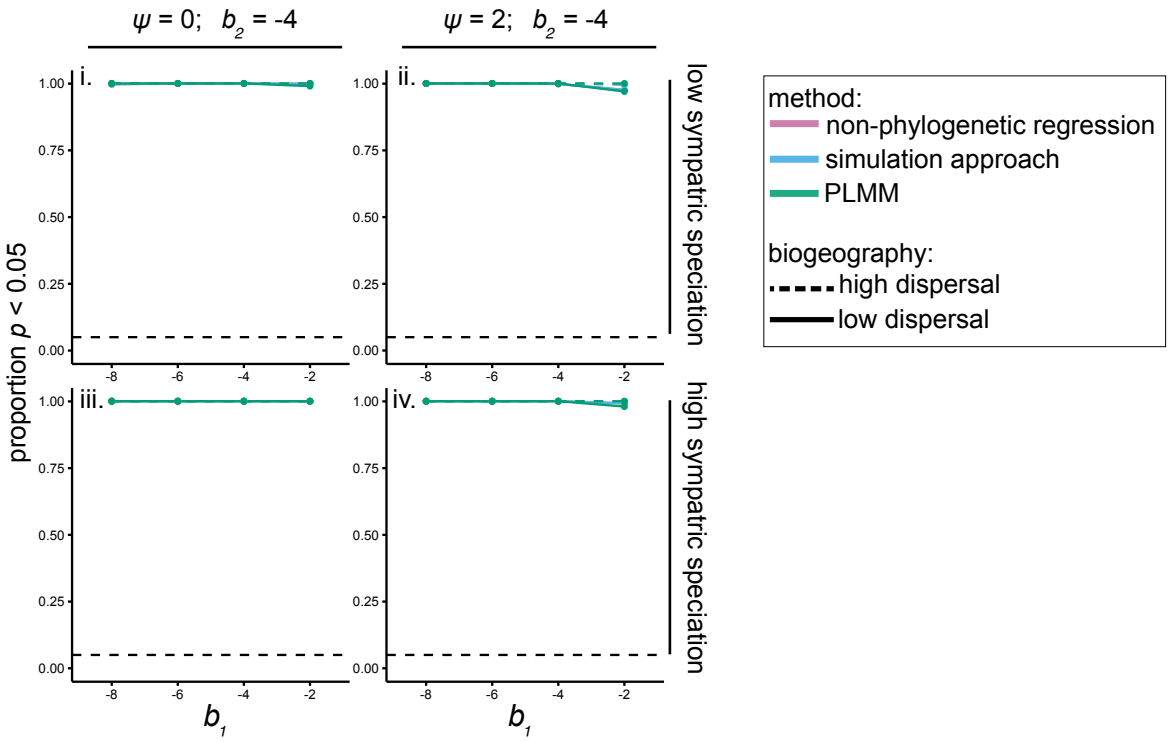

Supplementary Figure 17. The power to detect a causal relationship between a species interaction and similarity in a trait value is not affected greatly by varying the coefficient determining the strength of this relationship, regardless of whether the OU process is absent (i, iii) or present (ii, iv) in the measured trait. In these simulations, tree size was held constant at 100 species.